Non-invasive assessment of oxidative stress using ultraweak photon emission

バイオフォトンを用いた酸化ストレスの非侵襲的評価

The United Graduate School of Veterinary Science

Yamaguchi University

Katsuhiko TSUCHIDA

September 2021

TABLE OF CONTENTS

LIST OF FIGURES AND TABLES

CHAPTER 1

CHAPTER 2

CHAPTER 3

CHAPTER 4

ABBREVIATIONS

BCC: Basal cell carcinoma

CCD: Charge-coupled device

CAD: Canine atopic dermatitis

DHA: Docosahexaenoic acid

DHICA: 5,6-dihydroxyindole-2-carboxylic acid

DNA: Deoxyribonucleic acid

ECM: Extracellular matrix

ESR: Electron Spin Resonance

EtOH: Ethanol

IPD: Immediate pigment darkening

LC: Langerhans cell

MDA: Malondialdehyde

MMP: Matrix metalloproteinase

NADH: Nicotinamide adenine dinucleotide

NADPH: Nicotinamide adenine dinucleotide phosphate

8-OHdG: 8-hydroxy-2'-deoxyguanosine

PA: Protection grade of UVA

PMT: Photomultiplier tube

ROS: Reactive oxygen species

SC: Stratum corneum

SCC: Squamous cell carcinoma

SOD: Superoxide dismutase

SPF: Sun protection factor

UPE: Ultraweak photon emission

UV: Ultraviolet

UVA: Ultraviolet A

UVB: Ultraviolet B

CHAPTER 1: General introduction

1.1. Structure and function of human skin

Living organisms give off ultraweak photon emissions (UPE) in their biochemical reaction processes, also known as biophoton. They are spontaneously generated from the skin's surface and observed from human skin [1].

Human skin is the largest organ in the body, covering an area of approximately 1.6m^2 in adults [2]. Skin has the important function of maintaining the body's homeostasis. The structure of human skin is highly complicated, containing roughly three layers: the epidermis, the dermis, and subcutaneous tissue. 95% of the cells present in the epidermis are keratinocytes. The remaining 5% are composed of melanocytes, Langerhans cells (LC), and others. The stratum corneum (SC) is made up of keratinocytes in the epidermis. As the outermost layer of the skin, it has the essential function of preventing water evaporation, blocking foreign matter infiltration, and protecting the body from the external environment, which includes ultraviolet (UV) rays. The dermis contains the extracellular matrix (ECM) — along with collagen and elastic fibers — and blood vessels, sweat glands, sebaceous glands, and hair follicles. The boundary between the epidermis and the dermis shows an undulating structure, and the parts where the dermis protrudes toward the epidermis are called the dermal papillae. Subcutaneous tissue mainly consists of adipose tissue. It is responsible for heat insulation and the storage of

triglycerides.

1.2. Ultraviolet rays and human skin

Three types of electromagnetic waves — infrared, visible, and ultraviolet (UV) rays — reach the surface of the earth as sunlight. Among these, UV is known to have a significant effect on the human body [3]. It has the shortest wavelength and the highest energy among the electromagnetic waves reaching the surface of the earth [4]. UV is divided into UVA (320 to 400 nm), UVB (280 to 320 nm) and UVC (190 to 280 nm). The classifications correspond to the biological impact of each wavelength. UVC does not reach the surface of the earth because it is absorbed and scattered by the ozone layer in the upper atmosphere. Therefore, the types of UV that the living body is actually affected by are UVA and UVB.

It is well known that UV affects the skin, and it is thought that UV exposure from sunlight causes damage to the skin [5, 6]. UVA reaches deeper into the skin than UVB because of its wavelength. It is known that exposure to UVA for long periods of time accelerates skin aging (decrease in elasticity). It also has the effect of changing the light-colored melanin pigment in the epidermis into a darker color, temporarily darkening the skin (immediate pigment darkening [IPD]) [7]. UVA generates reactive oxygen species

(ROS) by exciting photosensitizers in the skin [8]. UVB causes an acute inflammatory erythema reaction in human skin, provoking an immediate skin reaction known as sunburn [9]. Sunburn is derived from the apoptosis of keratinocytes in the epidermis, suggesting the involvement of ROS generated by UV irradiation. Delayed tanning is observed in post-inflamed skin due to the increased production of melanin by UVB-activated pigment cells (melanocytes). On the other hand, UVB is also involved in the production of vitamin D in the skin, which regulates the homeostasis of calcium in the body [10].

The age-related skin changes common to UV-exposed areas of the body are unlike normal intrinsic aging. This is referred to as photoaging [5, 11]. Photoaging is thought to be induced by long-term UV exposure, and in general, the skin is histologically thickened, with visible flattening of rete pegs and dermal papilla. In the dermis, degeneration called solar elastosis — where elastic fibers become denser — is often observed. The involvement of metalloproteinases in the degeneration of elastic fibers and collagen fibers has been reported [12]. It has also been reported that the numbers of LC decrease in photoaged skin [13].

UV exposure is associated with skin cancer. Increased exposure to UV largely coincides with rising rates of cutaneous melanoma, and keratinocyte skin cancer which is comprised

of basal cell carcinoma (BCC) and squamous cell carcinoma (SCC) [14]. Therefore, it is now generally accepted that UV is one of the major causes of skin cancer [15].

1.3. Oxidative stress and skin

ROS play an important role in sustaining human life [16, 17], but when they are in excess, they damage cells and tissues and are thought to trigger illness and aging. Therefore, various mechanisms (antioxidant ability) for scavenging ROS are at work in the body [18]. In the living body, substances such as superoxide dismutase (SOD), glutathione and catalase act as antioxidants to eliminate and neutralize oxidative stress. When excess ROS that cannot be completely removed is generated, nucleic acids, proteins and lipids are oxidized, resulting in damage to their structure and function. When ROS exists in excess — and generation and elimination are imbalanced — this is called oxidative stress.

ROS refers to oxygen molecules and their related molecular species, which are more chemically reactive than oxygen molecules in the steady state [19]. ROS can broadly be divided into radical species with unpaired electrons and non-radical species without unpaired electrons. Radical species include superoxide anion ($O_2^{\bullet -}$) and hydroxyl radical ($^{\bullet}OH$). Non-radical species include hydrogen peroxide (H_2O_2) and singlet oxygen ($^1O_2$). ROS is produced endogenously by intracellular mitochondria and induced externally by

radiation or UV exposure. In the case of ultraviolet rays, singlet oxygen is also produced in addition to superoxide. Hydroxyl radicals and singlet oxygen have a short lifetime but are highly reactive.

In humans, oxidative stress is also involved in skin diseases including skin cancer and skin aging [20-23]. Therefore, it is very important to evaluate oxidative stress. Oxidative stress leads to chronic inflammation and skin cell dysfunction, and also contributes to skin diseases including cancer [23]. In human skin aging, oxidative stress plays a major role for intrinsic and extrinsic aging [20]. Extrinsic aging is attributed to the oxidative stress caused by UV irradiation.

In canines, the relationship between oxidative stress and atopic dermatitis has been reported [24, 25]. In addition, previous study on canine atopic dermatitis (CAD) showed that there are higher plasma malondialdehyde (MDA) levels in CAD patients than in healthy dogs and a highly positive correlation between the CADESI (Canine Atopic Dermatitis Extent and Severity Index) score and the plasma MDA in CAD patients. This suggests that oxidative stress with increased lipid peroxidation could be involved in the pathogenesis of CAD [24].

Further, radiation therapy used in cancer treatments is found to physically generate ROS, and this oxidative stress attacks cancer cells to exert an antitumor effect. However, since

oxidative stress may also occur in normal cells, measures must be taken following radiotherapy [26]. Experiments with rats have shown a relationship between radiation-induced skin damage and oxidative metabolites [27]. Oxidative stress assessment is also needed in medical and veterinary fields, as radiation therapy is performed not only in humans but also in animals.

1.4. Evaluation method for oxidative stress

Methods for evaluating oxidative stress include direct measurement of ROS, the measurement of oxidative stress markers, and the measurement of antioxidants. Some ROS can be directly measured by Electron Spin Resonance (ESR) requiring spin trapping agents [28]. Products produced by ROS, which are oxidative stress markers, include 8-hydroxy-2'-deoxyguanosine (8-OHdG) [29], carbonyl protein, and lipid peroxide. Also, antioxidant markers include SOD, glutathione, and catalase [30]. These oxidative stress markers can be measured relatively easily and are often used for oxidative stress evaluation, but reagents and extraction processes are required for these evaluations. These methods are useful for samples collected from living organisms and cultured cells. However, collecting samples of oxidative stress from humans or animals for in vivo analysis induces a burden, so non-invasive methods are required.

1.5. Evaluation of oxidative stress by ultraweak photon emission (UPE)

As an evaluation method that does not burden the living body, a method using UPE has been reported [31, 32]. UPE is an extremely weak spontaneous luminescence observed in living organisms, also referred to as the “biophoton” [33]. Of particular importance is that it is spontaneously expressed without any physical or chemical stimulus or manipulation, including artificial light or heat. UPE requires a dark environment due to its extremely weak light, but it can be detected using a photomultiplier tube (PMT) or a high-sensitivity charge-coupled device (CCD) camera [1, 31]. Since these methods can detect UPE from objects without contact, they are considered non-invasive and non-labelling. Artificial stimuli (UV irradiation and heat) induce increased UPE generation from plant seeds and skin [34, 35].

UPE is distinguishable from the phenomenon known as bioluminescence which occurs in fireflies and luminescent bacteria. Bioluminescence is light given off by species that have luminescent mechanisms based on enzymatic reactions. On the other hand, UPE mainly originates from ROS and free radicals generated in biochemical reactions. It is derived from the generation of excited molecules in the oxidation process by the ROS and free radicals. UPE is universally observed in all living organisms regardless of species. Figure 1.1 shows the emission intensity levels of UPE in comparison with visible light

intensity. The emission intensity is very weak, about 10^{-16} W / cm^2 (10^3 photon / s / cm^2) or less, which is about 3 to 6 orders of magnitude weaker than the intensity perceptible to the naked eye.

UPE is the luminescence emitted when the excited molecular species generated during biochemical reactions transition to the ground state [33]. Most of them usually originate from the oxidation reaction in the living body and are generally observed in the oxidation and peroxide processes of biological substances with ROS and free radicals. Taking the lipid peroxidation reaction as an example, ROS generated in the living body acts as an initiator to generate peroxy radicals, and excited carbonyl molecules and excited singlet oxygen are formed (Figure 1.2). It is presumed that these excited molecular species and biological substances excited by energy transfers become luminescent species. It has also been reported that it can be used to evaluate oxidative stress in living organisms through these light-emitting mechanisms. UPE have also been observed from human and animal skin and are used to evaluate oxidative stress in the skin. In addition, application in the evaluation of tumors in mice has been reported [36].

Photon counting using a PMT can be mentioned as a photon detection method, but it is also possible to image using an ultrasensitive cooled CCD camera [37]. An important characteristic of the use of UPE is that it can be measured non-invasively and without

labeling, which enables direct evaluation in vivo — a point of difficulty in the past. In addition, CCD camera imaging can visually capture the level of oxidative stress of the skin. Pigment darkening, delayed tanning, and erythema are examples of UV-induced skin changes that can be visually confirmed, but it is necessary to expose them to relatively large UV doses. On the other hand, UPE can be detected with a relatively small UV dose to the skin, so it is also useful in that it can evaluate the acute oxidative stress caused by UV without inducing a burden on the subject.

1.6. History of UPE research

In the 1920s, Gurwitsch suggested that ultraweak photons transmit information in living systems [38]. It was based on evidence found in experiments with onion roots as the “source” and “detector” [39]. Gurwitsch claimed that the growing tissues of one onion could induce or at least trigger the growth of a nearby specimen, it was called “mitogenetic radiation” (light found in visible and UV wavelength regions) [40]. Some experiments were conducted to confirm the reproducibility but the physical methods at the time didn't produce clear evidence for the existence of mitogenetic radiation [41] and interest in this subject declined in following decades.

In the1950s, the presence of biological radiation was re-examined with the development

of the photomultiplier tube (PMT) [42]. In the 1960s–1970s, studies were performed on the UPE of cells and tissues [43-46]. The development of the measurement apparatuses needed to detect UPE from biological samples was started in the 1970s [47, 48] and highly sensitive PMT was developed for biological applications [49] in the1980s. In the 1980s–1990s, two-dimensional photon counting cameras were able to detect that dividing tissues emit more than inactive neighbors [50]. Wounded parts were found to present a higher UPE than intact tissues [51, 52]. Moreover, it is commonly agreed that plant, animal, and human cells emit UPE — often referred to as biophoton [53-57]. Since the 2000s, UPE imaging systems have been further developed and used for spatiotemporal analysis, enabling the detection of fast changes in the UPE profile in response to stress [58]. In addition, according to the progress of scientific grade charge-coupled device (CCD) cameras, UPE of not only humans but also mice and insects have been observed in vivo using cryo-cooled CCD camera imaging systems [36, 59].

In this way, UPE has a long history of research from the confirmation of its phenomenon to the development of detection methods [60-62].

1.7. Thesis objectives

Although UPE measurement has the potential to replace other methods in that it can

evaluate skin oxidative stress non-invasively, it is not widely used as a general-purpose method. In order to investigate the potential of UPE detection for the skin, it is necessary to understand the phenomenon in more detail. Many things are still unclear regarding the mechanism of UPE generation from skin, and detailed studies are required to elucidate its application in evaluating the skin's oxidative stress. If the sources and mechanisms of UPE from skin are understood, it may be used as a valuable, non-invasive diagnostic method for both human and animal skin in the future.

Therefore, this thesis's objectives were to verify the usefulness of UPE measurement for the evaluation of oxidative stress in skin and to elucidate the mechanism.

Figures

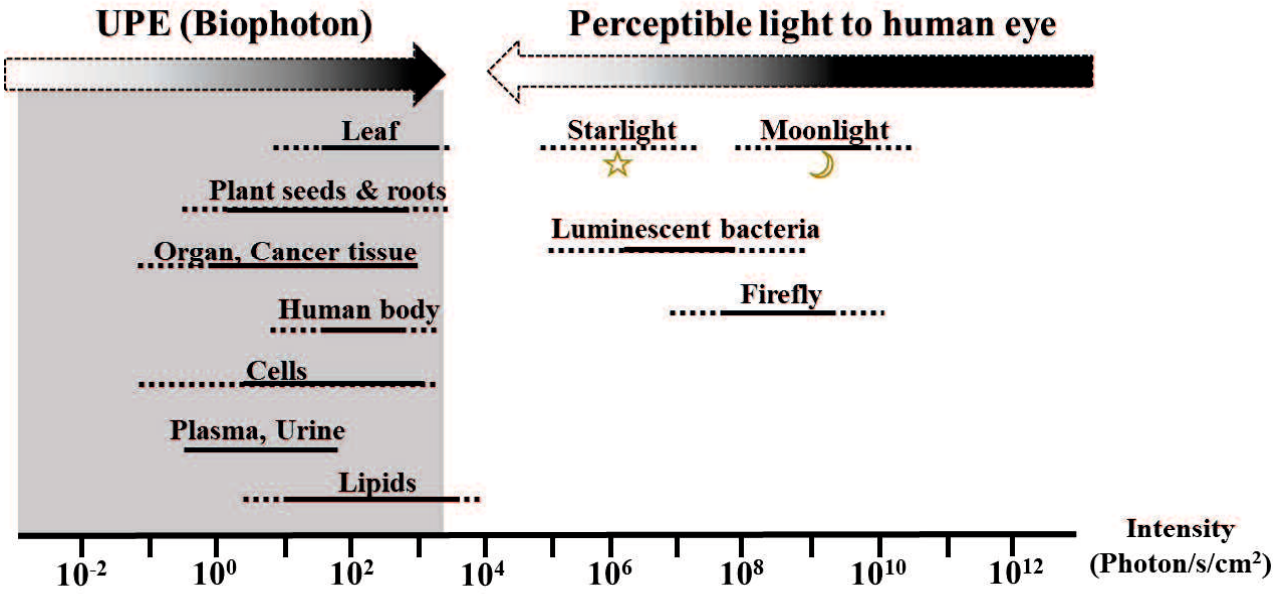

Figure 1.1. Emission intensity level of UPE

The emission intensity of UPE is much weaker than starlight, moonlight, or bioluminescence. It is about 3 to 6 orders of magnitude weaker than the intensity perceptible to the naked eye.

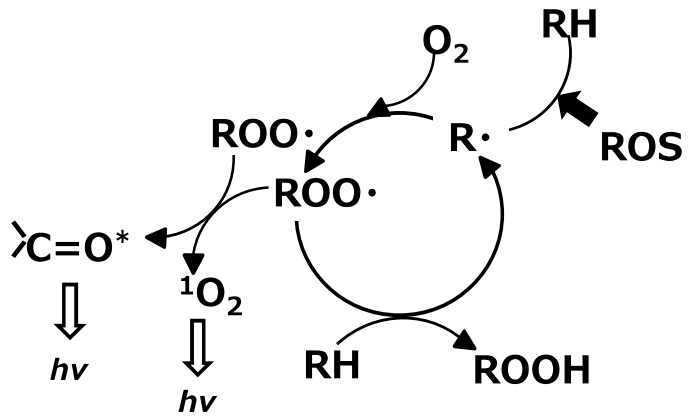

Figure 1.2. Mechanism of UPE generation in lipid peroxidation

Using the lipid peroxidation reaction as an example, ROS acts as an initiator to generate peroxy radicals, and excited carbonyl molecules and singlet oxygen are formed. The excited molecular species and biological substances excited by energy transfers are presumed to be luminescent species.

CHAPTER 2: Evaluation of UV-induced oxidative stress in human skin using ultraweak photon emission

2.1. Introduction

Living organisms [32, 33] — including microorganisms, plants, and humans [63, 64] — give off ultraweak photon emission (UPE) as a result of their biochemical reactions. This emission is often designated as the "biophoton". Presently, UPE measurement is used to evaluate oxidation stress and can potentially be used to perform optical biopsies to detect tumor viability [36]. UPE is detectable from human skin, and its intensity increases with external stress, such as with ultraviolet (UV) irradiation [31, 65, 66]. It was proposed that the electronically excited species responsible for UPE are formed by reactive oxygen species-induced lipid peroxidation and protein and nucleic acid oxidation [33]. The oxidation of these biomolecules leads to the formation of high-energy intermediates [67]. The decomposition of these intermediates generates electronically excited species that undergo electronic transition. UPE is accompanied by electronic transition from singlet-excited or triplet-excited states to the ground state. UPE intensity is extremely weak at approximately 10^{-16} W/cm^2 (10^3 photon/s/cm^2) or less, which is 1/1000th the sensitivity of the human eye. UPE can be distinguished from black-body radiation because the black-body radiation is 1/1000th the strength of UPE intensity [68].

UPE from human skin can be visualized using highly sensitive cooled charge-coupled device (CCD) cameras [69], offering a label-free and non-invasive method for detecting

oxidation.

In daily life, UV irradiation causes various skin complications. UV irradiation leads to increased ROS production [70, 71], which alters gene and protein functions [72]. This results in dysregulation of intracellular and extracellular homeostasis causing impaired skin function. ROS can interact with intracellular and extracellular components, thus causing oxidative reactions. It is well known that UV irradiation induces skin oxidation, as indicated by the squalene oxidation [73], protein carbonylation in the stratum corneum (SC) [74], and protein oxidation [75]. UV irradiation has also been reported to induce UPE from the skin. However, the mechanism of UPE generation has not been studied in detail. If better understood, evaluations of UPE from the skin may help in replacing the present methods used for evaluating oxidative stress of the skin.

In this chapter, experiments were conducted to confirm the characteristics and source of UPE generated from the skin, along with UPE's usefulness in the evaluation of skin oxidative stress. Additionally, the UV-protective efficacy of sunscreen using imaging technique was examined.

2.2. Material and Methods

2.2.1. UV irradiation

UV irradiation was generated using a Dermaray 200 (Canon Medical Supply, Tokyo, Japan) system with a UVA source (TOREX FL20SBL/DMR, 300–430 nm, peak 352 nm; Toshiba Medical Supply, Tokyo, Japan) and a UVB source (TL20W/12 RS, 280–380 nm, peak 311–313 nm; Phillips, Eindhoven, The Netherlands). UVA and UVB intensities were measured by DMR-UV-ABBNB-1 (Gigahertz-Optik GmbH, Puchheim, Germany).

2.2.2. Human skin tissue

Human (Caucasian) skin samples were purchased from Biopredic International (Rennes, France) and Analytical Biological Services (Wilmington, DE) via KAC (Kyoto, Japan). Subcutaneous tissues were removed prior to the experiments. The epidermis and dermis layers were obtained from the skin tissue by heating at 60°C. Human stratum corneum (Caucasian) sheets were purchased from Biopredic International (Rennes, France) via KAC (Kyoto, Japan).

2.2.3. UPE measuring systems

Imaging system:

UPE images were captured using a CCD camera system [69] in a dark chamber (Figure 2.1). The skin tissues were placed on the stage, and the human hands were inserted through an input port in vivo. UPE images were continuously taken with 5-min exposures using the CCD camera (SI 850s; Spectral Instruments Inc., USA, equipped with e2v CCD42-40). A specially designed high-throughput lens system was equipped. Imaging was performed on a surface area of 75 × 75 mm. In this experiment, the CCD was operated in the 8 × 8 binning mode, and the actual pixel number was 256 × 256. The resulting images were edited using ImageJ (NIH) and UPE intensity was calculated.

Spectroscopy system:

UPE spectra of excised human skin were taken using a polychromatic spectrum analysis system, which consists of a transmission-type diffraction grating, a lens system, and a CCD camera (SI 600s; Spectral Instruments Inc., USA) [76]. The exposure time of the CCD camera for spectral measurement of UV-induced UPE was set at 20 min. The exposure time for spontaneous UPE was set at 30 min and its photon intensity was multiplied by 2/3 to compare with the intensity of UV-induced UPE. UPE spectra were

measured by placing the skin tissue samples (n = 3) in a dark chamber containing the CCD camera.

2.2.4. UPE imaging of human skin

To evaluate the UV dose dependence of UPE, human skin was irradiated with various doses of UVA or UVB. To confirm the origin of UPE, human skin was separated into epidermis and dermis layers. The separated layers (epidermis and dermis) of human skin and human stratum corneum were irradiated with UVA (1,100 mJ/cm^2, 2.3 mW/cm^2) or UVB (234 mJ/cm^2, 0.65 mW/cm^2), and UPE images were immediately taken.

Once human skin was separated into the epidermis and dermis layers, the epidermis was placed on the dermis. After UVA (1,100 mJ/cm^2, 2.3 mW/cm^2) or UVB (234 mJ/cm^2, 0.65 mW/cm^2) irradiation to this reconstructed skin, human skin was separated into epidermis and dermis layers again, and the images of UPE generated from dermis layers were immediately taken.

To evaluate the effects of antioxidants against UV-induced UPE, 5% antioxidant solutions of sodium L-ascorbate (Kanto Chemical), L-glutathione (Sigma-Aldrich) and d-δ-tocopherol (Tama Biochemical) were prepared. Sodium L-ascorbate and L-glutathione solutions were prepared with PBS (−), whereas d-δ-tocopherol solution was

prepared with 50% EtOH. After UVA (1,100 mJ/cm^2, 2.3 mW/cm^2) or UVB (234 mJ/cm^2, 0.65 mW/cm^2) irradiation, 5% antioxidant solutions were applied to the skin surfaces (SC side), and UPE images were immediately taken.

2.2.5. UPE from human skin in vivo

After recruitment, human subjects (Asian, 7 healthy males in their 20s) provided written informed consent to participate in the study. Before measurement, subjects were asked to wash their hands. Subsequently, they were asked to wait for 10 min in a dark room to allow decrease in the effect by external light. Spontaneous UPE images of the skin at the back of fingers were taken for 5 min. The backs of the fingers were exposed to UVA at 800 mJ/cm^2 (1.33 mW/cm^2) via a SiO_2 plate with or without a sunscreen (SPF 50+, PA++++) coating (2 mg/cm^2). Irradiated skin areas measured 1 × 1 cm^2. Immediately after UVA irradiation, UVA-induced UPE images of the skin at the back of fingers were taken for 5 min.

2.2.6. Statistical analysis

Tukey–Kramer test was used for UPE images of each skin layer directly irradiated with UV and paired *t*-test was used for other experiments. The level of significance was

defined as *$p < 0.05$, **$p < 0.01$, and ***$p < 0.001$.

2.3. Results

2.3.1. Imaging of UV-induced UPE in human skin tissue

Intensities of UV-induced UPE were increased in a dose-dependent manner (Figure 2.2), clearly representing a reaction of skin to UVA and UVB. The data in Figure 2.3 show that UV-induced UPE was detectable from the epidermis and dermis, and intensity from the dermis was higher than that from the epidermis. UVA induced higher UPE in the dermis than UVB. In addition, UV-induced UPE from the stratum corneum was confirmed. After UV irradiation to the reconstructed skin with the epidermis placed on the dermis, UV-induced UPE was detected from the dermis but the intensities were lower than intensities that UV were irradiated to dermis directly (Figure 2.4). The lower intensities indicated that the epidermis partially absorbed UV radiation.

Figure 2.5 shows the effects of antioxidants against UV-induced UPE. UV-induced UPE was suppressed by antioxidant treatments confirming that UV-induced UPE are related to the oxidative stress of skin. The present antioxidant solutions did not emit UPE and did not absorb UV-induced UPE (data not shown).

2.3.2. Spectral patterns of UV-induced UPE

Polychromatic spectrum analyses revealed that UV irradiation induces UPE within the visible spectrum from the skin (Figure 2.6). Irradiation with UVA or UVB led to a similar peak UPE at approximately 550 nm. Spectral pattern of spontaneous UPE (non-irradiated skin) peaked at 600–650 nm. These experiments were performed in the visible range and UPE in the infrared range was not considered.

2.3.3. Suppression of oxidative stress by sunscreen in vivo

UVA-irradiated areas of finger skin showed UV-induced UPE, whereas UVA irradiation through sunscreen failed to increase the intensity of UPE (Figure 2.7). Because the sunscreen was indirectly applied, these data indicate actual UV protection by the sunscreen. Accordingly, UV-induced UPE significantly differed ($p < 0.01$) between parts with and without sunscreen.

2.4. Discussion

UV causes skin disorders via oxidative stress. To study these skin disorders, better methods of evaluating oxidative stress are required. In this chapter, the characteristics of UV-induced UPE in human skin were confirmed, along with its usefulness for evaluating

oxidative stress.

In UPE imaging, acute changes in UPE intensity were observed following UV irradiation, and these were dependent on the UV dose. Dose-dependent increases of photon counts following UVA irradiation have been identified in previous research [31]. In Figure 2.3, it showed that each skin layer (SC, epidermis and dermis) includes components that emit UV-induced UPE. Moreover, the results showed that UVA induced higher UPE in the dermis than UVB. It is proposed that UVA can oxidize the dermis more than UVB under sunlight because the UVA/UVB intensity ratio of sunlight is higher than that of our experimental condition [77]. Furthermore, it was indicated that UV-induced UPE from human skin includes UPE from not only the epidermis but also the dermis layer (Figure 2.4) and that the epidermis attenuates UV intensity. Considering the transmittance of UV to skin [78, 79], it is presumed that the contributions of the dermis against the total induced UPE is approximately 60%–80% for UVA and 20%–40% for UVB. Also, the contribution of the epidermis against the total induced UPE is approximately 20%–40% for UVA and 50%–70% for UVB. Differing contributions of UVA and UVB are reasonable because the transmittance of UVA to the dermis is higher than that of UVB.

Several studies reported that antioxidants suppress UPE photon counts [66, 80-82]. UPE imaging in this study also showed that three different antioxidants (sodium L-ascorbate,

L-glutathione, and d-δ-tocopherol) suppress UV-induced UPE. It supports the view that UPE is associated with oxidative stress. As the hydroxyl radical and superoxide anion radical induce more UPE [83], it is speculated that these antioxidants suppress UPE by radical-scavenging. Also, considering that imaging was performed immediately after applying antioxidant solutions, it is suggested that the antioxidant's effects were mainly observed in the epidermis.

Spectral patterns of spontaneous and UVA-induced UPE from human skin agree with previous studies [76, 84]. The spectral pattern of UVA-induced UPE peaked at approximately 550 nm and UVB-induced UPE showed a similar peak with UVA-induced UPE. Several researchers have reported the origin of UPE from human skin. The origin of UV-induced UPE was previously shown to comprise spectra from $^{3}(R=O)^{*}$ in the near UVA, blue–green regions (350–550 nm), and singlet- and triplet-excited pigments in the green–red region (550–750 nm) [33]. Additionally, it is assumed that the human skin includes the components where UV-induced UPE originate. Mei's group proposed the contribution of amino acids (predominantly tryptophan) excited by oxidation as being considered the major source of UPE [84]. Ou-Yang's group reported that the UVA-induced chemiluminescence may largely be attributed to the breakdown of dermal collagen cross-links [85].

It was shown that photosensitization reactions can oxidize lipids and proteins in the skin [86]. The chromophores in the skin absorb UVA and UVB, and the absorption of UV radiation by the chromophores leads to the formation of an excited state of the photosensitizer. Following this, the oxidation of biomolecules results in the formation of triplet-excited carbonyl [$^3(R=O)^*$] and singlet oxygen ($^1O_2$) via type I or type II reactions, which emit photons in the visible wavelength region. Also, components such as collagen and melanin [87, 88], which can be excited, are proposed as a source of UV-induced UPE in the visible wavelength region. For instance, it is suggested that alteration of the cross-links of collagen by UV irradiation [89] induces ROS via a photosensitization reaction and that the pigments such as melanin [76] may cause photon emission through energy transfer from triplet-excited carbonyl.

Finally, the in vivo test shows that sunscreen protects against UV. Previously, protection of skin from UVA by sunscreen was determined by measuring the photon count [35]; however, the antioxidant effect of sunscreen can be visually evaluated using imaging systems. This data led us to conclude that UPE imaging is a useful method for evaluating the oxidative stress of the skin, along with a sunscreen's antioxidant effects. Imaging with the CCD camera was less sensitive than photon counting using PMT but it provided the advantage of visual evaluation of the skin's oxidation stress.

The study in this chapter confirmed the source of UV-induced UPE in the skin and the usefulness of oxidative stress evaluation by UPE. Assessing oxidative stress on the skin is very important in medical and veterinary fields, as oxidative damage occurs not only in humans but also in animals. Among the many evaluation methods, evaluation using UPE is non-invasive, and it is very promising because it can be performed without imposing a burden on the living body. In this study, acute oxidation by UV exposure was focused on, but it is expected that chronic oxidation can also be adequately evaluated.

Figures

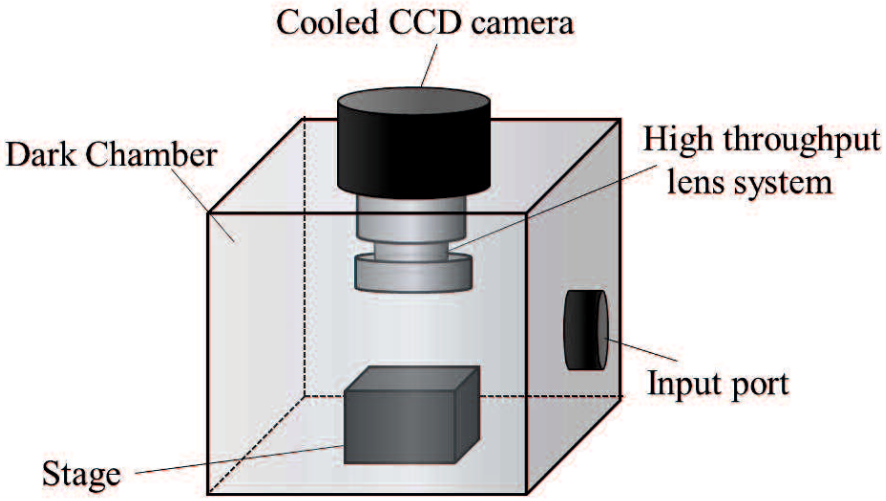

Figure 2.1. Schematic illustration of UPE imaging system

The skin tissue was placed on the stage. The hand was inserted through an input port and the finger was set under the CCD camera. UPE were captured using a CCD camera.

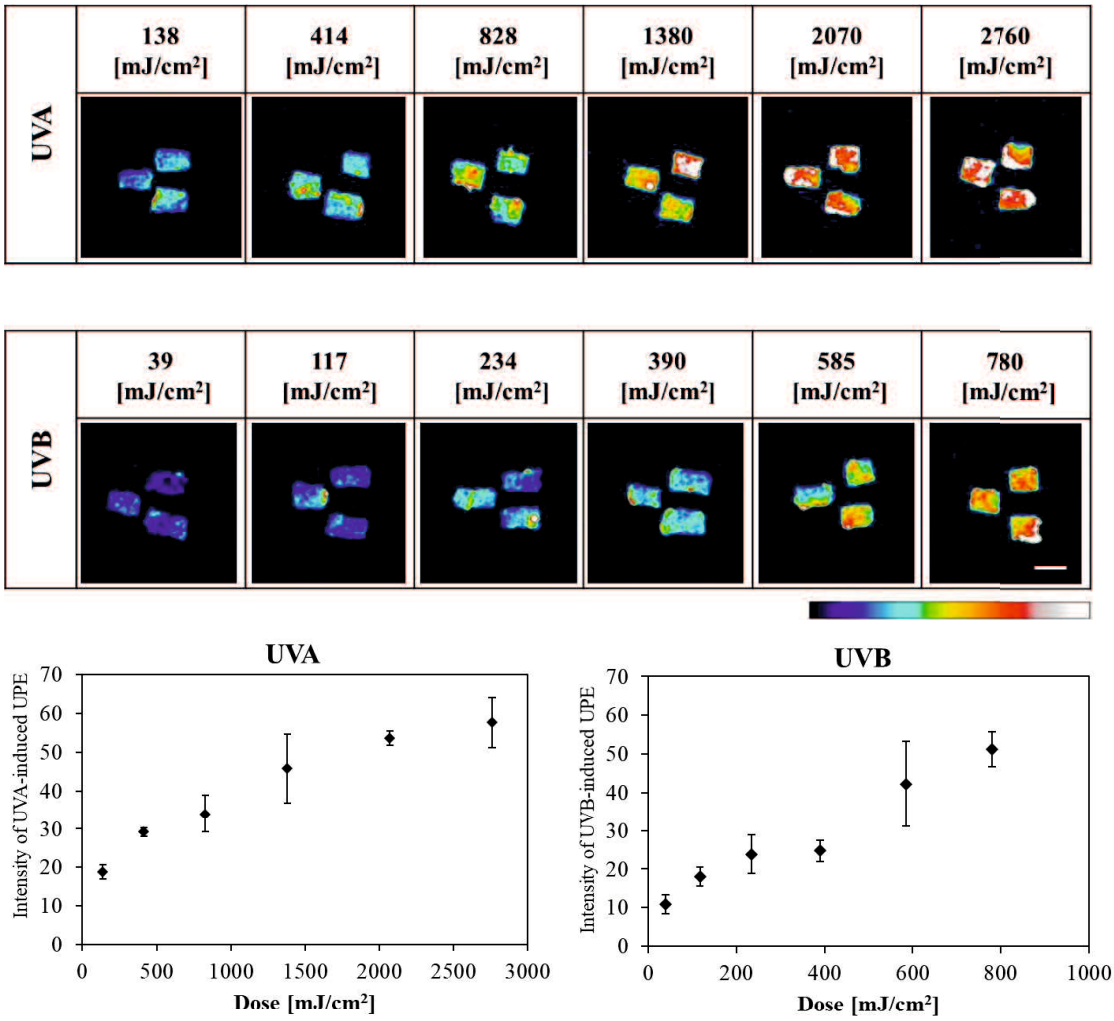

Figure 2.2. UV-induced UPE originating from human skin tissue

Human skin tissue was irradiated with several doses of UVA or UVB. UPE images were captured using a cooled CCD camera with 5-min exposures; scale bar, 1 cm. The color scale indicates signal intensity from 0 (blue) to 100 (white). The graph shows intensity of UV-induced UPE determined from imaging data. The intensity of spontaneous UPE (non-irradiated skin) was subtracted. Graphed data are presented as means ± SD, n = 3.

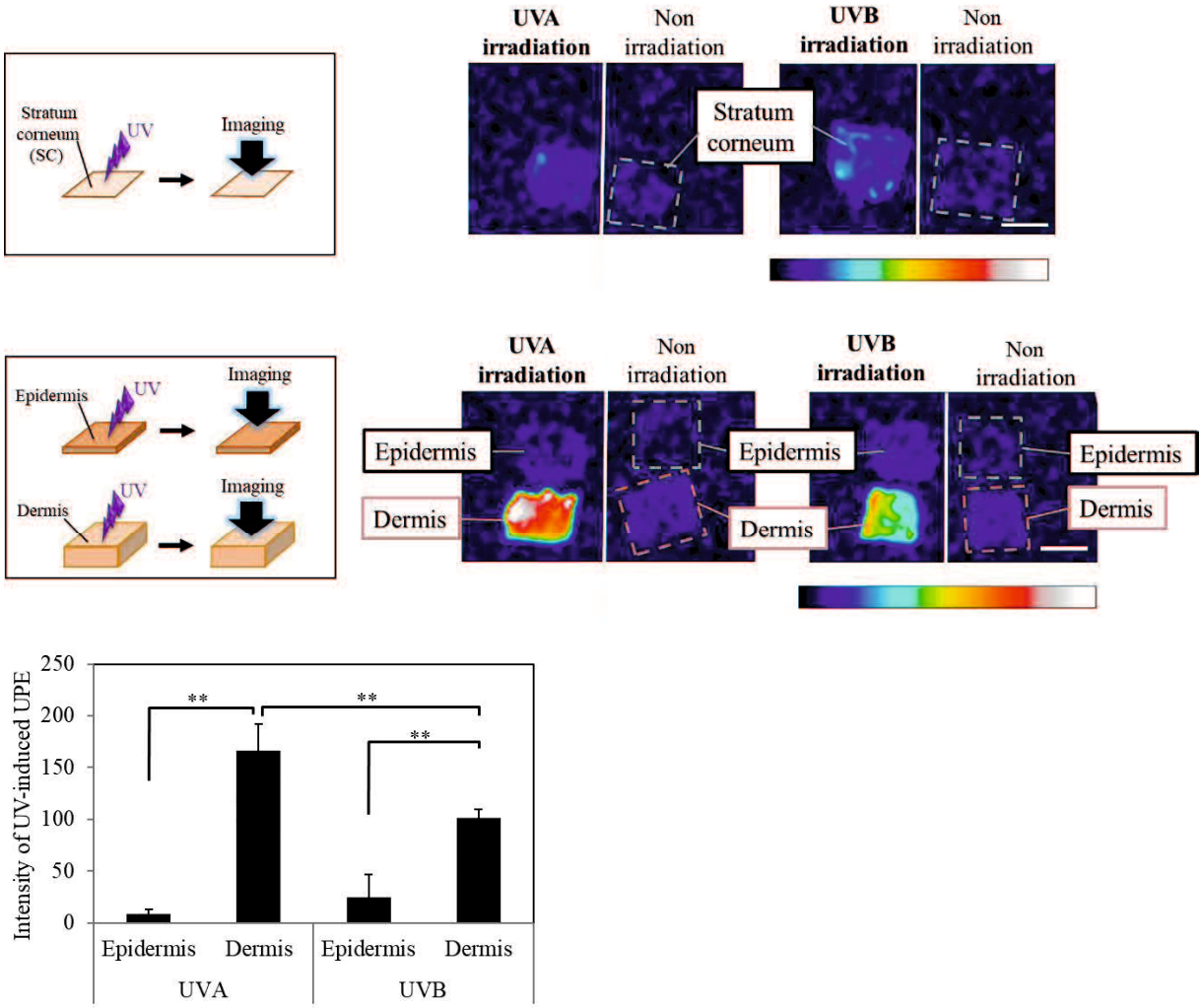

Figure 2.3. UV-induced UPE from SC, epidermis and dermis layers

Separated skin layers were irradiated with UVA (1,100 mJ/cm^2) or UVB (234 mJ/cm^2). UPE images were captured using a cooled CCD camera with 5-min exposures; scale bar, 0.5 cm. The color scale indicates signal intensity from 0 (blue) to 280 (white). The intensity of UV-induced UPE is determined from the imaging data and is shown in the graph. Graphed data are presented as means ± SD, (UVA) n = 5, (UVB) n = 4; $^{**}p < 0.01$. The intensity of spontaneous UPE (non-irradiated skin) was subtracted.

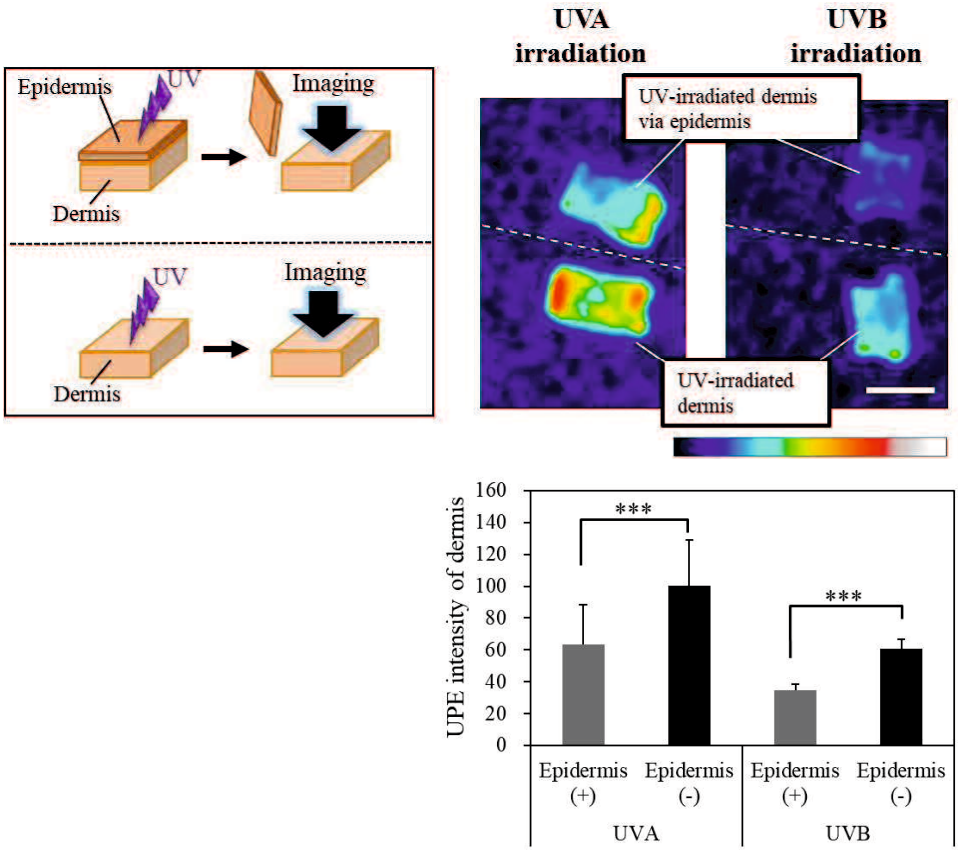

Figure 2.4. UPE from dermis after UV irradiation via epidermis

Dermis samples with or without overlying epidermis were irradiated with UVA (1,100 mJ/cm^2) or UVB (234 mJ/cm^2). The upper portions of the images show dermis after UV irradiation via epidermis [Epidermis (+)]. The lower portions of the images show dermis that was directly irradiated by UV [Epidermis (−)]. Imaging data were taken using a cooled CCD camera with 5-min exposures; scale bar, 0.5 cm. The color scale indicates signal intensity from 0 (blue) to 280 (white). Graphed data are presented as means ± SD, n = 4; ***$p < 0.001$.

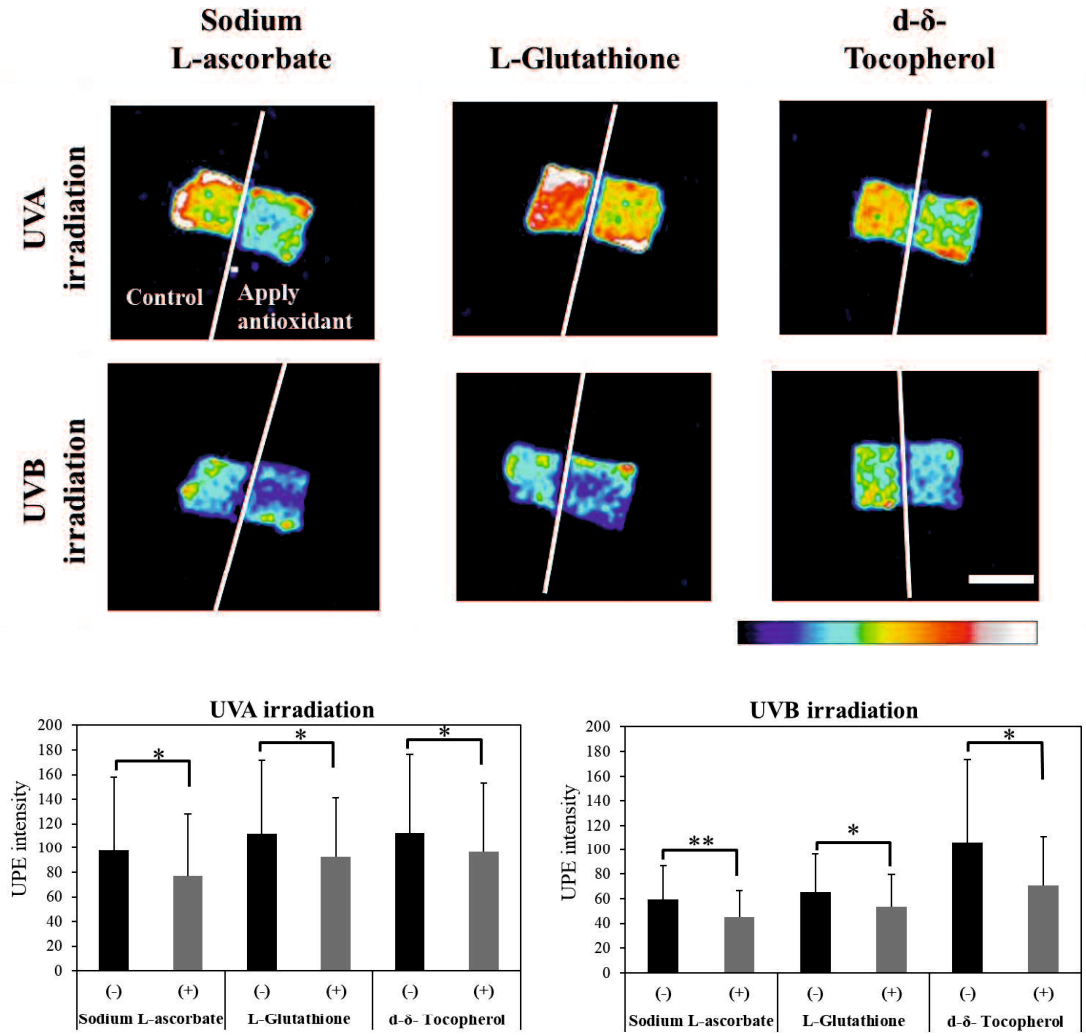

Figure 2.5. The effect of antioxidants against UV-induced UPE

Human skin tissues were irradiated with UVA (1,100 mJ/cm^2) or UVB (234 mJ/cm^2). After UV irradiation, antioxidants were applied to the right sides of skin tissues and the respective solvents were applied to the left sides of skin tissues. Imaging data were taken using a cooled CCD camera with 5-min exposures; scale bar, 1 cm. The color scale indicates signal intensity from 0 (blue) to 100 (white). Graphed data are presented as means ± SD, n = 5; *$p < 0.05$, **$p < 0.01$.

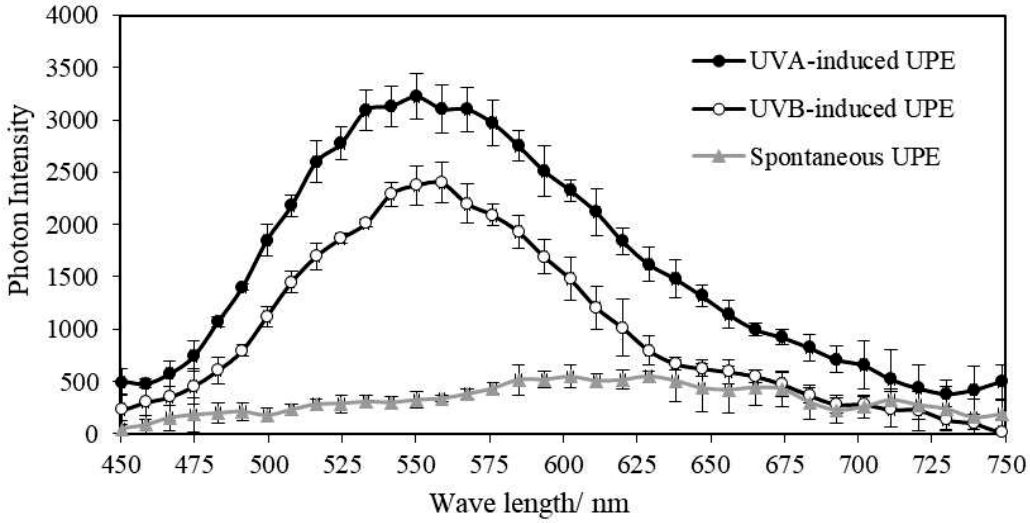

Figure 2.6. Spectrum of UV-induced UPE in human skin tissue

UPE spectra were taken for 20 min after irradiating human skin tissue with UVA (1,100 mJ/cm^2) or UVB (234 mJ/cm^2). The spectrum of spontaneous UPE was taken for 30 min and its photon intensity was multiplied by 2/3. The black line with closed circles shows UPE spectra after UVA and the black line with open circles shows spectra after UVB. The gray line indicates spontaneous UPE from human skin tissue (non-irradiated skin). Data are presented as means ± SD, n = 3.

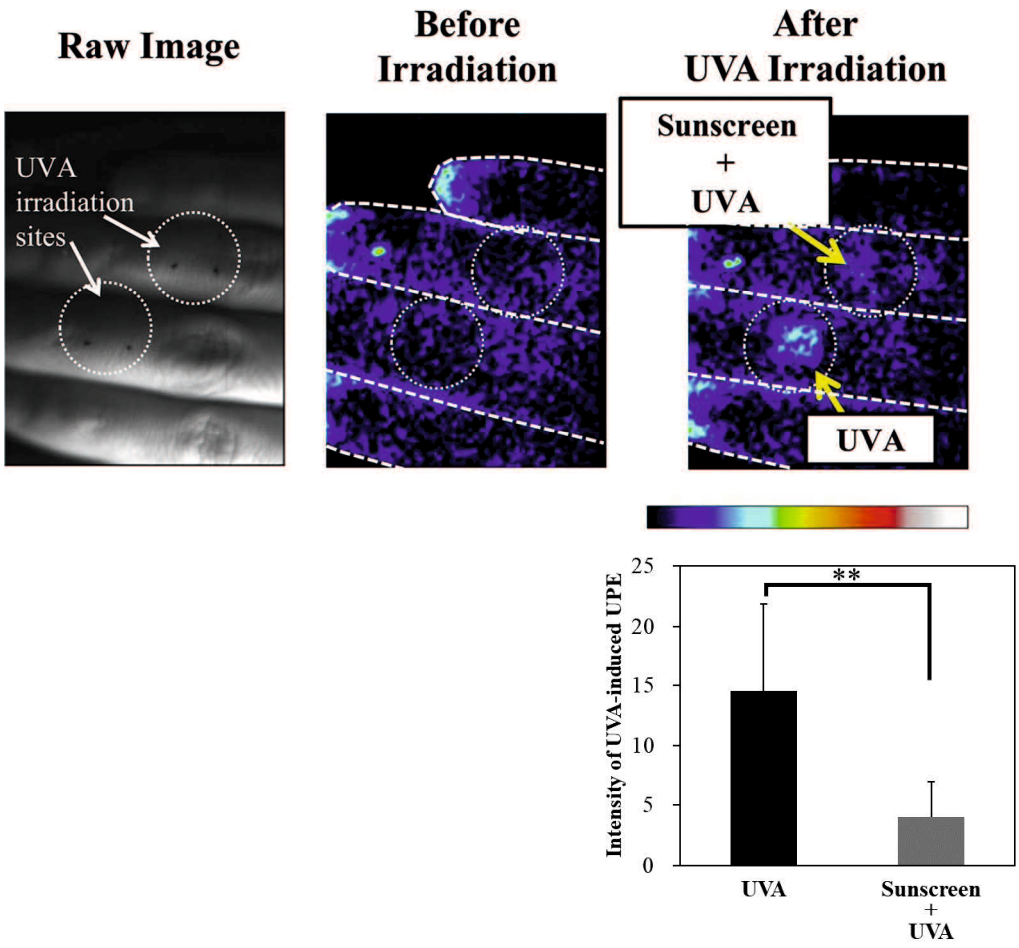

Figure 2.7. Imaging of UV protection by sunscreen in vivo

UVA was applied to the backs of fingers at 800 mJ/cm^2 via a SiO_2 plate with or without sunscreen coating. Imaging data were taken using a cooled CCD camera with 5-min exposures. The color scale indicates signal intensity from 0 (blue) to 100 (white). The graphed data show that sunscreen suppresses UV-induced UPE intensities. Graphed data are presented as means ± SD, n = 7; $^{**}p < 0.01$. The intensity of spontaneous UPE (non-irradiated skin) was subtracted.

CHAPTER 3: Chronic oxidative stress in human facial skin observed by ultraweak photon emission imaging and its correlation with biophysical properties of skin

3.1. Introduction

Oxidative stress can cause skin wrinkling and is known to be associated with skin diseases in humans. It has been suggested to play a role in the pathogenesis of human skin cancers [90]. Reactive oxygen species (ROS) are involved in the pathogenesis of several allergic and inflammatory skin diseases [21]. ROS can alter gene and protein function [72] to dysregulate intracellular and extracellular homeostasis, thereby impairing skin function. The mitochondria, along with enzymatic reactions in the cell, are major source of ROS [91, 92]; in addition UV radiation also induces ROS production. UV radiation can cause skin complications by increasing ROS production [70, 71], and by oxidizing squalene [73, 93] and other proteins [75]. Moreover, carbonylated protein levels in the stratum corneum of the skin are correlated with the skin's physiological parameters [74].

Oxidative stress in the skin is conventionally measured using methods that require labelling with various molecules [94]. These were invasive and non-direct methods to investigate skin oxidation. However, ultraweak photon emission (UPE), also known as the biophoton, was recently used to assess oxidative stress in the skin non-invasively and directly.

UPE is generated by living organisms [32], including humans [63, 64]. The

electronically excited species responsible for UPE are formed during lipid peroxidation and ROS-induced protein and nucleic acid oxidation [33]. Therefore, UPE imaging can be used for non-invasive label-free evaluations of the oxidative stress in skin. UPE generated by the skin is visualized under highly sensitive, cooled, charge-coupled device (CCD) cameras [69]. An increase in UPE was demonstrated in cancer-implanted nude mice by imaging [36].

In the chapter 2, two-dimensional UPE imaging showed the usefulness in assessing acute oxidative stress in the skin caused by UV. This study demonstrated that UV-induced UPE is generated not only by the epidermis but also the dermis. Moreover, the spectrum of UV-induced UPE showed a peak in the visible range.

The face is a highly specialized component of the human body, and facial skin is exposed to various adverse environmental conditions, including UV light. The skin of the human face is chronically exposed to UV light, which causes photoaging [95]. While several studies have been conducted on facial skin, there are only a few reports on the oxidative stress of facial skin due to the limitations of conventional methods. Considering that the human face shows site-specific differences in biophysical properties [96, 97], regional variations of oxidative stress are predicted. Regional differences of blood flow, trans-epidermal water loss, stratum corneum hydration,

temperature, pH, and sebum content in the face have been reported. Additionally, with ageing, wrinkles around the eyes are characteristically observed [98].

In this chapter, the UPE of whole facial skin was measured to evaluated chronic oxidative stress. Moreover, age-related alterations in UPE in each facial site were examined, along with the relationship between UPE intensity and biophysical properties of the skin. Based on these results, the effects of oxidative stress on facial skin were discussed.

3.2. Material and Methods

3.2.1. Volunteers

Fifty healthy volunteers (Asian, female, aged 22–69 years) were enrolled in this study. The study was approved by the Ethics Committees of Shiseido Co. Ltd., and Tohoku Institute of Technology, all methods were carried out in accordance with the relevant guidelines and regulations, and written informed consent was obtained from all volunteers. The exclusion criteria for volunteers were severe atopy, allergies, sunburn, topical medication (except cosmetics), and other skin abnormalities in the face.

3.2.2. UPE imaging system

A highly sensitive, cooled, CCD camera (600 series, Spectral Instruments Inc., AZ, USA) coupled with a specially designed high-throughput lens system was used for imaging. A back-illuminated CCD (original pixel format: 2048×2048, pixel size: 13.5×13.5 mm; CCD42-40, Teledyne e2v, UK) and a closed-cycle mechanical cryogenic cooler were incorporated in the camera system. The lens system was specially designed to maximize the light collection efficiency for UPE imaging. The CCD camera was operated in the 16×16 binning mode, with the actual pixel number of 128×128 (spatial resolution: 1.6×1.6 mm).

Figure 3.1a shows the construction of the UPE imaging system for facial skin. The imaging system consisted of a dark room with double partitions, cooled CCD camera with lens, and head-chin rest for fixing the face. A compressor for cryogenic cooler and a monitor were set outside of the dark room. An air fan was installed to prevent changes in the temperature and humidity in the dark room. All measurements were performed at 15 min exposure time.

3.2.3. Measurement procedure

After washing the face with a facial cleanser to remove sebum from the surface

affected by the external environment prior to measurement, volunteers wore black cape from the neck down to prevent the effects of luminescence from their clothes. Volunteers were rested in the dark room for 15 min to prevent the effect of delayed luminescence caused by external light. Spontaneous UPE images of facial skin were captured for 15 min. Wrinkle scores and porphyrin scores in the face were analyzed using the VISIA system (VISIA Evolution, Canfield Scientific, NJ, USA) [99] which analyses biophysical properties of skin from color or UV photographs. Photographs of from the right and front sides of the face were taken. The photographs of right side were used for wrinkle analysis, while the ones of the front were used for porphyrin analysis. Wrinkle scores and porphyrin scores were calculated using factors such as the count, degree, and measurement area. Skin color parameters (L*, a*, b*) of the cheek were measured using the CM-700d spectrophotometer (Konica Minolta, Tokyo, Japan).

3.2.4. Image analysis

ImageJ software (National Institutes of Health, Bethesda, MD, USA) was used to analyze UPE images and measure UPE intensity. To remove noise from the images and blur them, the following features from the ImageJ software were applied: I. “Despeckle” and II. “Smooth”. The parts of black cape from the neck down were selected as

background, the background intensity was subtracted to calculate the actual UPE intensity of the skin. UPE intensities of the 16 defined facial regions (Figure 3.1b) were analyzed and the UPE intensities of the same areas on the left and right sides were averaged. Sites that showed abnormal luminescence were excluded from analysis. Therefore, the number of valid data for each part of the face was as follows: 1: Forehead (n = 50), 2: Area between the eyebrows (n= 50), 3: Nose (n = 50), 4: Area under the nose (n= 45), 5: Lip (n = 40), 6: Chin (n = 46), 7–8: Corners of eyes (n= 50), 9–10: Upper eyelids (n = 49), 11–12: Lower eyelids (n = 49), 13–14: Cheeks (n = 49), 15–16: Area around the nose (n = 50). To analyze the correlation between UPE intensity and biophysical properties, UPE intensities corresponding to measurement areas for evaluation of biophysical properties were averaged.

3.2.5. Statistical analysis

The Steel-Dwass test was used to verify the regional variations of UPE intensity in facial skin. The correlation between age or biophysical properties parameters, other than skin color and UPE intensity, was evaluated using Spearman's rank correlation coefficient. The correlation between skin color parameters and UPE intensity was evaluated using Pearson’s correlation coefficient.

3.3. Results

3.3.1. Regional variations in UPE intensity of facial skin

Photon emission from facial skin was captured in a dark room with double partition (Figure 3.1a). UPE image of the facial skin is shown in Figure 3.2. Regional variations in the UPE intensity were observed for different facial areas. As shown in Figure 3.1b, 16 facial areas were defined, and the UPE intensity of each area was calculated. Figure 3.3a shows the mean UPE intensity in each area for all volunteers. The intensities of area between the eyebrows, eyelids, nose, around and under the nose and lip were significantly higher than that of the chin ($^{*}p < 0.05$, $^{**}p < 0.01$). Among these area with higher UPE, the area between the eyebrows, the nose and around and under the nose showed even higher UPE intensity ($^{\dagger}p < 0.05$, $^{\dagger\dagger}p < 0.01$). Figure 3.3b shows the mapping of the UPE intensity normalized to that of the chin with the lowest intensity for relative comparisons.

3.3.2. Age-related variations in UPE intensity of facial skin

As shown in Figure 3.4a and Figure 3.4b, UPE intensities of the upper eyelids and areas around the corners of the eyes increased with age in 22-to-50-year-old volunteers. Furthermore, there were no age-related variations in the UPE intensity in 51-to-69-year-

old volunteers.

Figure 3.4c shows Spearman's rank correlation coefficient and *p*-value of each site in the face in the 22-to-50-year-old and in 51-to-69-year-old volunteers. No significant age-related changes in UPE were observed in the sites other than the upper eyelids and areas around the corners of the eyes.

3.3.3. Correlation between UPE intensity and biophysical properties

Figure 3.5 shows the relationship between UPE intensity and biophysical properties (e.g., wrinkling of skin, porphyrin). Wrinkle score around the right eyes significantly correlated with UPE intensity in 22-to-50-year-old volunteers (Figure 3.5a). However, there was no correlation between the above-mentioned parameters in 51-to-69-year-old volunteers (Figure 3.5b). Whereas porphyrin score was significantly correlated with UPE intensity in volunteers of all ages (Figure 3.5c), skin color parameters were not (L*, a*, b*; Figure 3.6).

3.4. Discussion

UPE imaging revealed regional variations of oxidative stress in human facial skin. Thereafter, the relationship between UPE intensity and the biophysical properties of

facial skin was investigated. Site-specific oxidation of facial skin may help elucidate the causes of various skin conditions and diseases. Moreover, site-specific oxidation of certain areas of facial skin is possible due to the oxidative stress caused by high levels of sebum [100, 101] and increased susceptibility to oxidative stress by exposure to UV light. Regional variations of antioxidant function in facial skin are also suggested to contribute to site-specific oxidation of facial skin.

In this study, chronic oxidation and its relationship with the biophysical properties of facial skin were examined. The vulnerability of the skin to oxidation could induce skin problems such as acne, rosacea, inflammation, and wrinkling. The results showed a positive correlation between skin wrinkling and UPE intensity. Several studies have reported the high incidence of skin cancer of the nose [102, 103], and the results in this study have shown that the nose is particularly susceptible to high oxidative stress. Furthermore, the role of oxidative stress in malignant melanoma and non-melanoma skin cancer [90], and oxidative-stress-associated carcinogenesis has been reported [104, 105]. Increased oxidative stress can result in a higher incidence of skin cancer; hence, UPE imaging may be used for the prognosis of skin cancer.

Age-related variations in UPE intensity were observed only in the skin areas surrounding the eyes. The skin surrounding the eyes is thinner than that in other regions

[106], and experiences mechanical stress during facial movements and cosmetic application/removal during everyday life. This site is exposed to ultraviolet rays in the sunlight. Therefore, it suggests that these functions with sun exposure cause age-related variations in UPE intensity and the oxidation induces wrinkling of the skin surrounding the eyes. It has been shown that ROS induces a decrease and degradation of the extracellular matrix (ECM) which is associated with wrinkling [107]. Additionally, previous reports established the relationship between skin wrinkling and oxidative stress using conventional methods such as surface shape evaluations and histological analyses [108, 109]. Moreover, in contrast with conventional indirect methods, the UPE method allows for direct evaluation of oxidative stress. In chapter 2, UV-induced UPE was shown to be generated not only in the epidermis, but also in the dermis. Further, it has been reported that ROS formation during the skin's metabolic processes contributes to spontaneous UPE from the skin [81]. Further, UPE derives from electronically excited species formed by ROS-induced lipid peroxidation, and protein and nucleic acid oxidation [33]. Considering the oxidative stress of the epidermis and dermis, it is reasonable to expect a correlation between skin wrinkling and UPE intensity.

UPE is also generated from UV-induced photosensitization reactions with photosensitizers such as porphyrins. This may explain the correlation between UPE

intensity and the score of porphyrins excreted by bacteria. The conventional method of detecting porphyrins requires the use of a Wood's lamp that emits long-wave UV radiation [110]. However, UPE detection may be useful to determine the levels of porphyrins without using UV radiation. Furthermore, porphyrin-induced oxidative stress is thought to be the major mechanism of porphyrin-mediated tissue damage [111]. Therefore, UPE-based detection methods can improve our understanding of porphyrin-related disorders. Finally, the a* value, which indicates skin redness, did not correlate with UPE intensity, although the relationship had been speculated because skin redness related to blood flow is affected by inflammation, which is related to the generation of oxidative stress [112]. This non-correlation is most probably due to the absorption of visible light by blood [113]. It is therefore vital to examine the contribution of biomolecules in the skin, including blood, to UPE generation to further understand the underlying mechanisms. Additionally, the association between UPE and skin color warrants further research since only the color of the cheeks was measured in this study.

In conclusion, UPE imaging of facial skin revealed regional variations of oxidative stress and site-specific increases in oxidative stress with age. Moreover, a correlation was found between oxidative stress and the biophysical properties of the skin. In particular, it is suggested that wrinkle formation on the face is influenced by oxidative

stress. This study may provide insights into the treatment of areas of facial skin that are vulnerable to aging. It also has the potential to improve our understanding of a variety of skin diseases. In conclusion, UPE measurement is useful and has great room for growth in the evaluation of both acute and chronic skin oxidation.

Figures

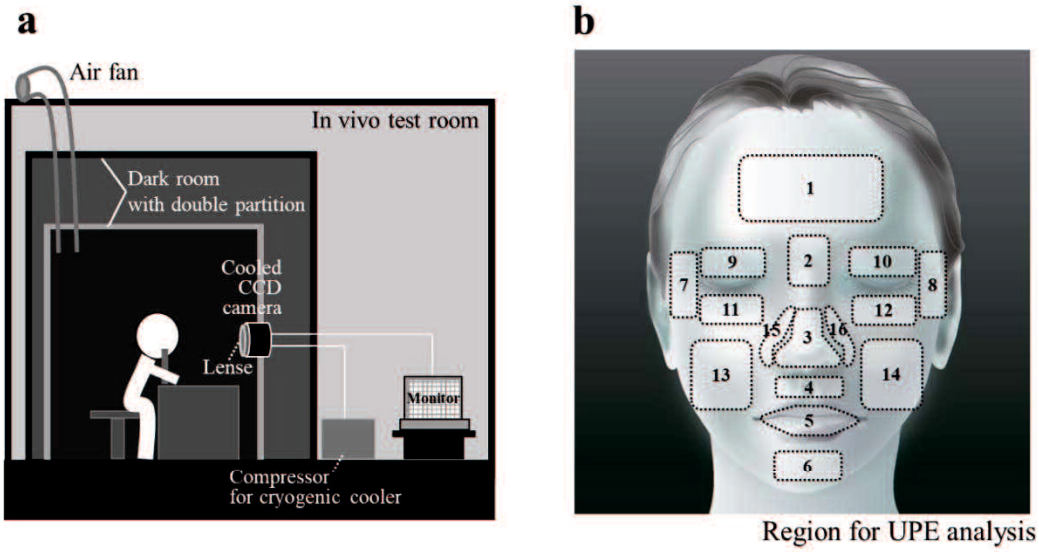

Figure 3.1. UPE imaging system for facial skin and UPE analysis sites

(a) UPE imaging system for facial skin in this study. Volunteers were rested in a dark room with double partition. UPE images of facial skin were captured using the cooled CCD camera for 15 min. (b) Facial illustration of the regions used for UPE analysis. Sixteen facial areas were defined and the UPE intensity for each area was calculated from the UPE images. 1: Forehead, 2: Area between the eyebrows, 3: Nose, 4: Area under the nose, 5: Lip, 6: Chin, 7–8: Corners of eyes, 9–10: Upper eyelids, 11–12: Lower eyelids, 13–14: Cheeks, 15–16: Area around the nose.

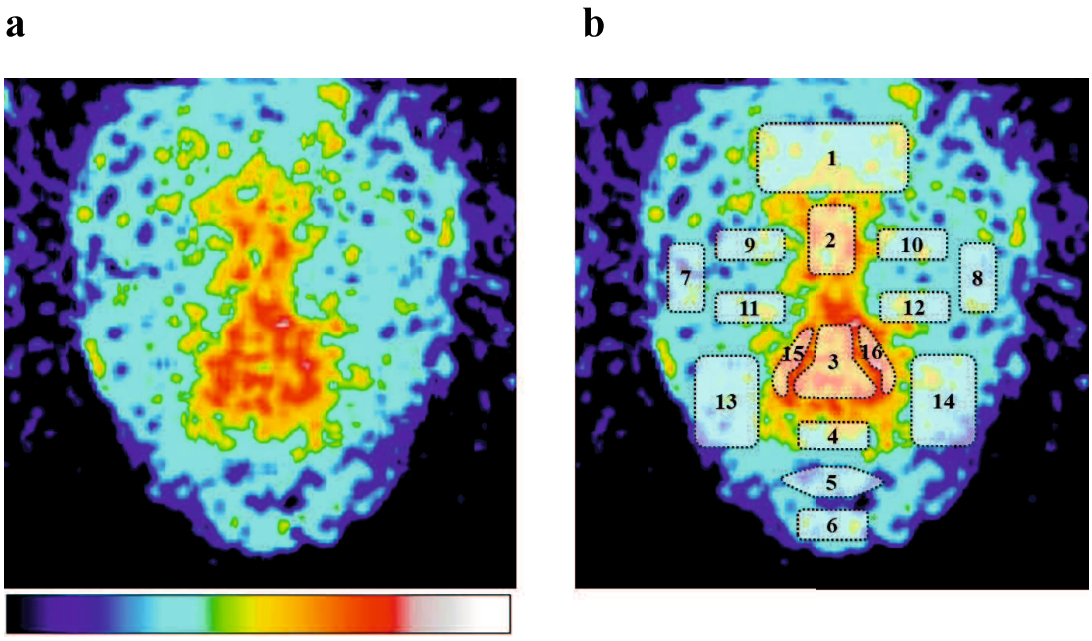

Figure 3.2. UPE image of facial skin

(a) Representative UPE image of facial skin. UPE imaging data were captured using a CCD camera with a 15-min exposure. The color scale indicates signal intensity from 0 (black) to 5.0 (white). (b) Merged UPE image of facial skin with the regions used for UPE analysis.

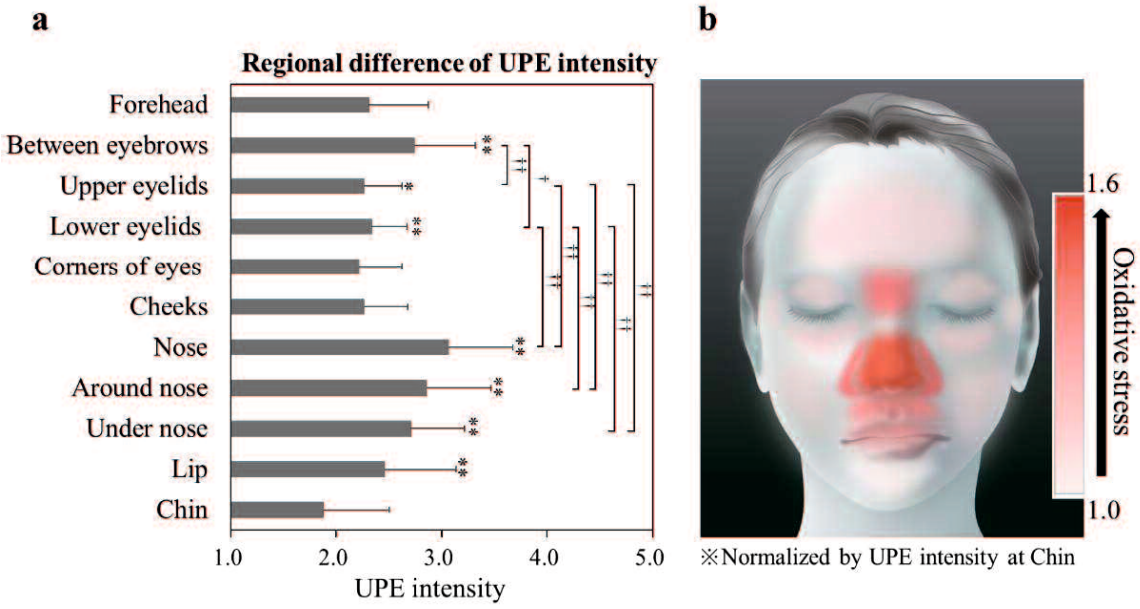

Figure 3.3. Regional variations of UPE intensity in facial skin and mapping of oxidative stress

(a) UPE intensity of each site was averaged for volunteers of all ages (22–69 years,) and UPE intensities of the same sites on the left and right sides were averaged. Data are presented as means ± SD, and the number of data of each site were as follows: Forehead (n = 50); area between the eyebrows (n = 50); nose (n = 50); area under the nose (n = 45), lip (n = 40); chin (n = 46); corners of eyes (n = 50); upper eyelids (n = 49); lower eyelids (n = 49), cheeks (n = 49); area around the nose (n = 50). $^{*}p < 0.05$, $^{**}p < 0.01$ vs. UPE intensity of the chin (Steel-Dwass test). There were significant differences in UPE intensity between sites with higher UPE ($^{\dagger}p < 0.05$, $^{\dagger\dagger}p < 0.01$ [Steel-Dwass test]). (b) Facial illustration showing the mapping of oxidative stress level normalized by UPE intensity of the chin.

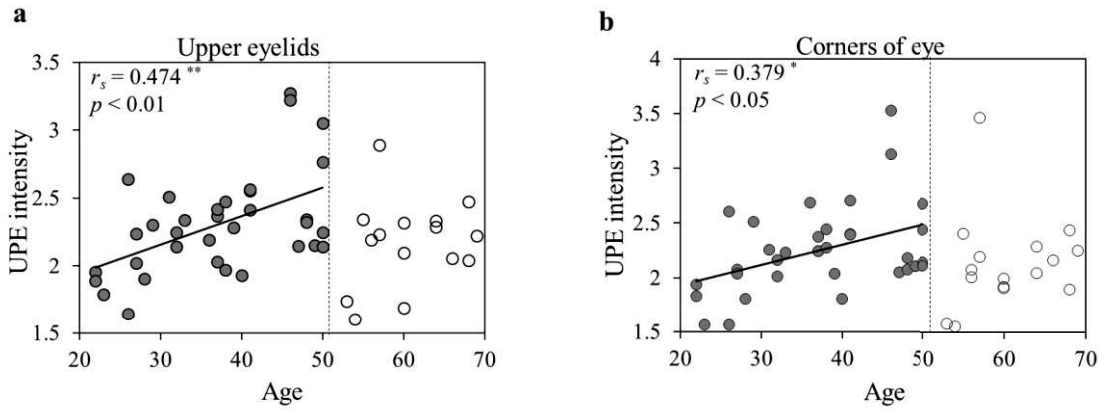

c

22 − 50 years	Spearman's rank correlation coefficient ; r_s	*p*-value	Number of data ; *n*
Forehead	0.301 ns	0.084	34
Area between eyebrows	0.250 ns	0.249	34
Nose	0.117 ns	0.502	34
Area under nose	0.076 ns	0.662	34
Lip	− 0.097 ns	0.609	29
Chin	0.119 ns	0.502	33
Corners of eyes	0.379 *	0.029	34
Upper eyelids	0.474 **	0.007	34
Lower eyelids	0.251 ns	0.149	34
Cheeks	0.036 ns	0.835	34
Area around nose	0.112 ns	0.520	34

51 − 69 years	Spearman's rank correlation coefficient ; r_s	*p*-value	Number of data ; *n*
Forehead	0.146 ns	0.571	16
Area between eyebrows	0.066 ns	0.798	16
Nose	0.043 ns	0.869	16
Area under nose	0.195 ns	0.537	11
Lip	0.055 ns	0.863	11
Chin	0.207 ns	0.472	13
Corners of eyes	0.291 ns	0.259	16
Upper eyelids	0.185 ns	0.489	15
Lower eyelids	0.235 ns	0.380	15
Cheeks	0.322 ns	0.228	15
Area around nose	0.053 ns	0.838	16

Figure 3.4. Relationship between age and UPE intensity of each site in the face

(a)(b) A correlation was observed between age and UPE intensity for upper eyelids or corners of the eyes in 22-to-50-year-old volunteers (closed circles) but there was no correlation in 51-to-69-year-old volunteers (open circles). (c) Spearman's rank correlation coefficient and *p*-value between age and UPE intensity of each site in the face in 22-to-50-year-old and in 51-to-69-year-old volunteers. ns: not significant, *: $p < 0.05$, **: $p < 0.01$ (Spearman's rank correlation test).

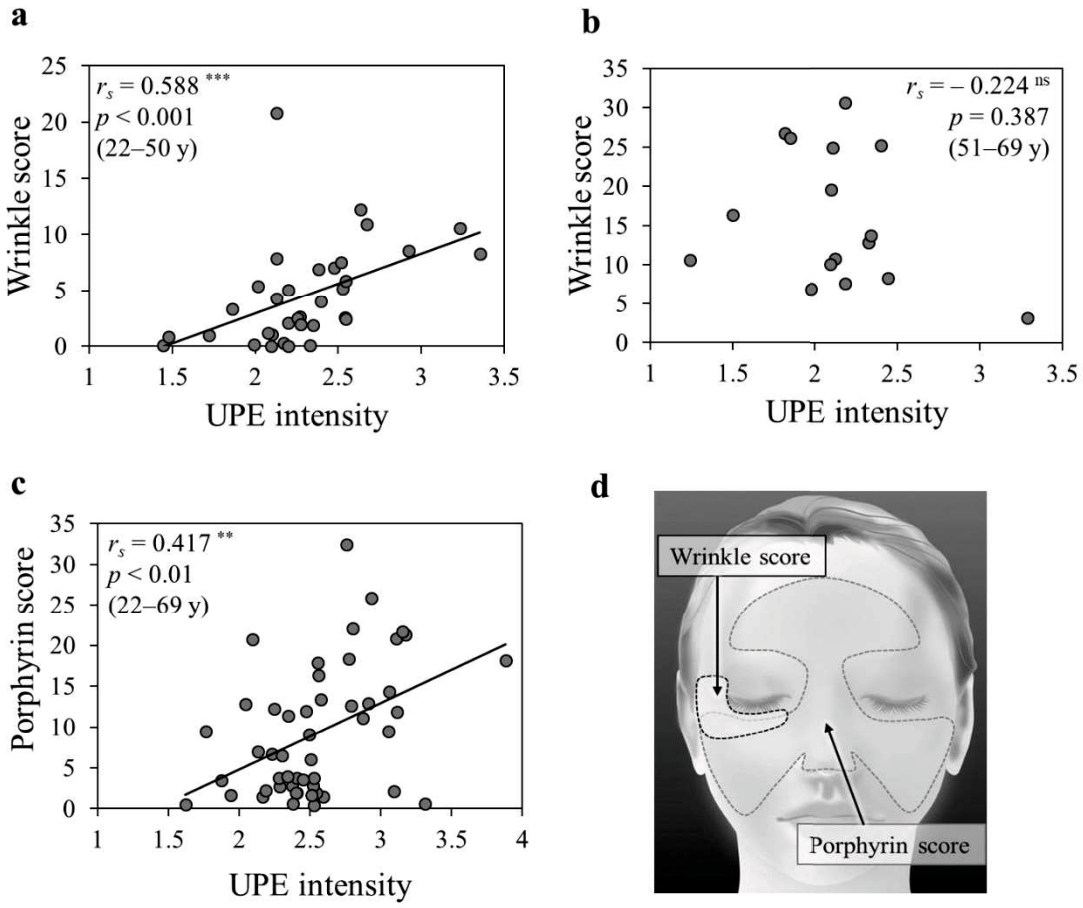

Figure 3.5. Relationship between UPE intensity and biophysical properties

(a)(b) UPE intensity correlated with wrinkle score around the right eyes in 22-to-50-year-old volunteers (n = 34) but there was no correlation in 51-to-69-year-old volunteers (n = 16). (c) UPE intensity correlated with the facial porphyrin score for volunteers of all ages (22–69 years, n = 50). (d) Facial illustration indicating measurement areas for wrinkle score and porphyrin score assessment. UPE intensity corresponding to measurement areas was averaged. ns: not significant, **: $p < 0.01$, ***: $p < 0.001$ (Spearman's rank correlation test).

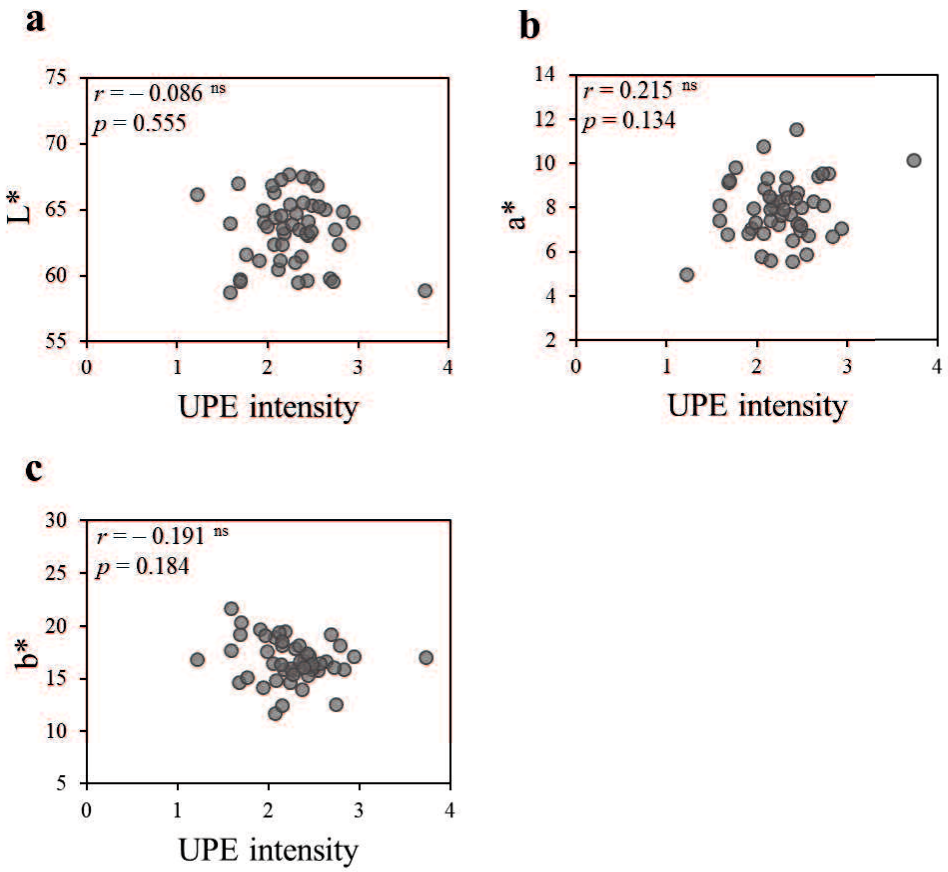

Figure 3.6. Relationship between UPE intensity and skin color parameters

There was no correlation between UPE intensity of the cheek (22–69 years, n = 49) and skin color parameters [(a) L* value, (b) a* value, (c) b* value]. ns: not significant (Pearson's correlation test).

CHAPTER 4: Polychromatic spectrum analysis of ultraweak photon emission induced from biomolecules

4.1. Introduction

Redox reactions continuously occur in the living body to regulate various physiological and cellular processes; among these, the oxidation reaction causes oxidative stress and is associated with various diseases when unregulated [114-116]. Oxidative stress has been recognized as a factor contributing to aging and progression of multiple neurodegenerative diseases [117]. Therefore, it is necessary to elucidate the mechanism of oxidation, for the development of anti-aging strategies and the treatment of related diseases.

The phenomenon of oxidation has also attracted attention in the field of dermatological research, since oxidative stress is associated with human skin photoaging and skin diseases [21, 112, 118]. Particularly, skin cancer is a serious problem in the dermatological field and is related to excessive levels of oxidative stress [90, 119]. Ultraviolet (UV) irradiation is a major generator of oxidative stress. Therefore, it is important to investigate the mechanism of oxidative stress in the skin caused by UV irradiation [120].

Many methods of evaluating oxidative stress have been developed to date. In vitro, oxidative stress is commonly assessed by measuring the levels of reactive oxygen species (ROS) in cells and of radicals in liquids using specific reagents [94]. In vivo,

transgenic mice expressing a redox-sensitive fluorescent protein have been used to assess oxidation in the skin [121]. In addition, oxidative stress can be detected using ultraweak photon emission (UPE) that is spontaneously generated in living organisms [32]. UPE, also referred to as biophoton, is an extremely weak luminescence emitted from the living body, including human, animals and plants [63, 64]. The human skin also exhibits UPE, which reportedly increases under exposure to UV irradiation [66]. UPE is considered to be derived from electronically excited species formed by ROS-induced lipid peroxidation and protein and nucleic acid oxidation [33]. The oxidation of these biomolecules leads to the formation of high-energy intermediates [67] and their decomposition generates electronically excited species. It has been reported that singlet oxygen ($^1O_2$) directly emits UPE, and other ROS, such as superoxide anion radical ($O_2^{\bullet -}$), hydrogen peroxide (H_2O_2), hydroxyl radical ($^{\bullet}OH$), are indirectly involved in the generation of UPE via the oxidation process and photosensitization reaction [33, 122]. The key advantages of using UPE for the evaluation of oxidative stress are that it is a label-free method and allows for non-invasive measurements in vivo.

The usefulness of UPE measurement in assessing oxidative stress has been reported before [31, 123]. In chapter 2 and chapter 3, it also showed that UPE measurements using a cooled charge-coupled device (CCD) camera is useful for assessing acute and

chronic oxidative stress in human skin. UV-induced UPE in the skin tissue was measured as acute oxidation and UPE of whole facial skin was measured in vivo as chronic oxidation. The UV-induced UPE from the skin decreased by applying antioxidants, showing that UPE derived from oxidative stress. In chapter 3, it proposed that oxidative stress is correlated with wrinkle formation and porphyrin scores in the skin, highlighting the importance of antioxidation measures in preventing skin damage induced by oxidative stress. The dermal layer has been proposed to be one of the sources of UPE in previous research [85] and chapter 2, suggesting that the measurement of skin UPE could reflect the degree of oxidative stress throughout the skin, including the epidermal and dermal layers. However, the UPE of biomolecules has not been sufficiently measured to explore the origin of UPE generation in the skin. Knowing the detailed origins of UPE will promote the evaluation of oxidative stress using UPE.

Spectral analysis is one of the main approaches to reveal the characteristics of UPE generation. A recent study showed that *Arabidopsis* subjected to mechanical injury exhibited enhanced photon emission, which led to changes in the spectral pattern [124]. Another study demonstrated a difference in the spectral patterns of UPE from the body surface between human breast cancer-bearing nude mice and healthy control mice

[125]. These studies demonstrate that spectral analysis is an essential component of UPE research. However, there has been no detailed investigation regarding the mechanism of UPE generation at the molecular level. Many endogenous fluorophores in the skin show a unique emission wavelength, which can be captured using two-photon microscopy [88]. Two-photon excitation occurs by the simultaneous absorption of two photons at infrared wavelengths, leading to the emission of a fluorescence photon. As the emission wavelength of the fluorescence photon in two-photon microscopy depends on the molecular species, it is expected that different biomolecules exhibit different UPE spectra. Based on this premise, in this chapter, the detailed emission source of UPE in the skin under exposure to UVA irradiation was investigated using polychromatic spectral analysis of the relevant biomolecules in the skin and a human skin tissue sample. Components that can be oxidized in the skin were selected as biomolecule samples. Elucidation of the characteristics of UPE generated during UVA irradiation can provide new insights into understanding the mechanisms contributing to skin photoaging and skin diseases, which can in turn offer new targets for treatment and prevention.

4.2. Material and Methods

4.2.1. Skin tissue samples

A human skin sample from the breast of a 58-year-old Caucasian female was purchased from Biopredic International (Rennes, France) via KAC (Kyoto, Japan) and stored frozen. The subcutaneous tissue was physically removed from the skin sample prior to UVA irradiation and spectral measurements. Three smaller pieces of skin tissue were prepared from the skin sample. Subsequently, all the three tissue pieces were, independently, irradiated with UVA, and the UPE spectra were measured. The skin tissue pieces that were UVA-irradiated once and used for spectrum measurement were not used again in the experiment.

4.2.2. Skin biomolecule assessment

The following seven biomolecules were selected for spectral analysis: phospholipids (solid, non-hydrogenated egg phosphatidylcholine; Coatsome NC-50, NOF Corporation, Tokyo, Japan), elastin (solid, from bovine neck ligament powder; E1625, Sigma-Aldrich, St. Louis, MO, USA), linoleic acid (liquid; 126-03612, Fujifilm Wako Pure Chemical Corporation, Osaka, Japan), linolenic acid (liquid, α-linolenic acid; 20526-52, Nacalai Tesque, Kyoto, Japan), collagen (solid, VitroCol lyophilized type I

collagen from human; 5008, Advanced BioMatrix, Inc., San Diego, CA, USA), 5,6-dihydroxyindole-2-carboxylic acid [DHICA] (solid, Tokyo Chemical Industry Co., Ltd., Tokyo, Japan), and whole blood (liquid, human heparin sodium whole blood; BioIVT, West Sussex, UK via KAC, Kyoto, Japan). For measurement, 1 mM DHICA was dissolved in 0.1 M phosphate buffer (pH 7.4), the whole blood was diluted 10-fold with Dulbecco's phosphate-buffered saline (−), and raw samples were used for the other molecules.

4.2.3. UVA irradiation

UVA irradiation was generated using a Dermaray 200 system (Canon Medical Supply, Tokyo, Japan) with a UVA source (TOREX FL20SBL/DMR, 300–430 nm, peak 352 nm; Toshiba Medical Supply, Tokyo, Japan). The UVA intensity was measured by DMR-UV-ABBNB-1 (Gigahertz-Optik GmbH, Puchheim, Germany). The skin tissue and each of the biomolecule samples were irradiated with UVA at 1100 mJ/cm^2, 2.3 mW/cm^2.

4.2.4. Spectroscopy

The UPE spectra of the human skin tissue and biomolecule samples were measured

using a polychromatic spectrum analysis system developed by Kobayashi et al. [76] (Figure 4.1), which consists of a transmission-type diffraction grating, condenser lens, collimator lens, input slit, and cooled CCD camera (SI 600s; Spectral Instruments Inc., USA). The detection wavelengths of this spectroscopy were in the range of 450–750 nm. Unlike spectroscopic devices that continuously detect UPE at each wavelength, the spectroscopic system used in this research detected UPE at each wavelength at the same time. Thus, there was no lag time in the detection of each wavelength.

The measurement procedure was as follows: The sample was irradiated with UVA outside the dark chamber. After UVA irradiation, the liquid biomolecule samples were immediately placed in a borosilicate glass cuvette, which was placed under a 1 mm wide and 20 mm high optical input slit in the dark chamber of the spectroscopic system. In contrast, solid biomolecule samples and the skin tissue were immediately set on the plate after UVA irradiation and placed directly under the input slit in the dark chamber. The skin tissue was placed with the stratum corneum facing the input slit. Immediately after UVA irradiation and sample placement, the spectrum was recorded. Exposure times for spectral measurement of UV-induced UPE were set to 20 min for the skin tissue and 5 min for the biomolecule samples. UPE intensities at each wavelength were normalized by the intensity at the peak wavelength and are expressed as the relative

intensity to facilitate direct comparisons. Spectra of the skin tissue and biomolecule samples were measured several times depending on the emission intensity to confirm reproducibility. Specifically, the skin tissues' spectra were measured three times, while those of linoleic acid, elastin, and linolenic acid were measured twice each, and for phospholipids and DHICA they were measured four times each.

4.3. Results

The UPE spectra from five of the seven biomolecules were successfully measured. However, the diluted blood and collagen samples did not exhibit UPE generation induced by UVA irradiation and therefore their spectra were not obtained. UPE intensities at each wavelength were normalized by the intensity at the peak wavelength and the average values were calculated for comparison. The UVA-induced UPE spectra of skin tissue and the individual skin biomolecules are shown in Figure 4.2 and Figure 4.3, respectively, revealing distinct spectral patterns. Specifically, the spectrum for skin tissue peaked at 550 nm, whereas the peaks of linoleic acid, elastin, phospholipids, linolenic acid, and 1 mM DHICA solution peaked at 475 nm, 525 nm, 570 nm, 575 nm, and 585 nm, respectively. For linoleic acid, the peak was close to the limit of detection (450 nm) of the spectroscopy system on the short wavelength side, suggesting that

photons with wavelengths shorter than 450 nm were likely included.

Table 4.1 shows the wavelength regions for the peak of each sample, which was defined as a relative intensity greater than 0.9. The peak of each biomolecule was within a 40–70 nm range, demonstrating broad peaks similar to the spectrum of the skin tissue. Table 4.1 also shows the UPE intensities (counts/min) at the spectral peak wavelength. UPE intensity at the spectral peak for the skin tissue was 160 (550 nm), whereas that for linoleic acid, elastin, phospholipids, linolenic acid, and 1 mM DHICA solution was 2760 (475 nm), 10930 (525 nm), 1230 (570 nm), 5610 (575 nm), and 320 (585 nm), respectively.

4.4. Discussion

The oxidation of biomolecules has been suggested to impact several key functions in the living body, including the ones in skin. Therefore, it is important to understand the oxidation potential of each biomolecule for inferring the causes of biological changes and oxidation-related diseases. In the present study, comparisons of UVA-induced UPE generation in the entire skin and from individual biomolecules found in the skin that are considered to be strongly affected by oxidation revealed clearly different peaks and wavelength ranges for each biomolecule. The UPE intensity of biomolecules depends

on the sample size, and the biomolecular weight used in this study does not match the amounts that are actually present in the skin.

A series of lipid oxidation reactions that give rise to various products [126] may contribute to the spectral range, but since there are further complex contributions, further studies are needed. Linoleic acid (C18:2) has just one less double bond than linolenic acid (C18:3); however, their UPE spectral patterns are remarkably different from each other. This finding suggests that double bonds may majorly contribute to the emission wavelengths of UPE. An in vitro study showed that linoleic acid hydroperoxide, which is formed under oxidative stress, increased the levels of pro-matrix metalloproteinase (MMP)-1 in cultured arterial endothelial cells and increased the levels of both proMMP-1 and proMMP-3 in cultured smooth muscle cells [127]. MMPs are involved in processes such as tissue remodeling and degradation of the extracellular matrix containing collagen and proteoglycans. Similarly, linoleic acid hydroperoxide was shown to significantly increase the production of MMP-1 and MMP-3, suggesting that lipid peroxides are able to alter collagen metabolism [128]. Another study showed that the expression level of MMP-1 increased in fibroblasts after UVA irradiation and sun exposure contributed to the formation of facial wrinkles [129]. Collectively, these findings suggest a relationship between UV-light-induced lipid

peroxidation and wrinkle formation. Indeed, the study in chapter 3 confirmed a relationship between oxidative stress and wrinkle formation in facial skin. α-Linolenic acid accumulates in the bodies of mammals (carcass, adipose, and skin) and its major metabolic route is beta-oxidation. A small proportion of ingested α-linolenic acid is converted to docosahexaenoic acid (DHA) [130], which has been shown to improve skin wound healing in rats [131]. Due to these beneficial effects of DHA produced by the oxidation of linolenic acid, it is relevant to investigate the oxidation of linolenic acid.

The UPE wavelengths obtained in the present study for elastin and phospholipids were similar to their reported fluorescence emission ranges [87, 132]. UV-irradiated elastin was previously shown to produce hydrogen peroxide [133] and oxidation was reported to cause structural changes to elastin [134]. The effects of oxidized phospholipids suggest their potential relevance in different pathologies, including atherosclerosis, acute inflammation, lung injury, and many other conditions [135]. In contrast to elastin and phospholipids, the UPE wavelength region of DHICA, a melanin precursor [136], was slightly longer than the reported fluorescence range of melanin [88] and tyrosine [87], a known DHICA precursor [136]. DHICA oxidized by $^1O_2$ loses the capacity to induce DNA damage [137]. Considering the fluorescence lifetime [138], UPE is

different from fluorescence emission as it has a longer emission lifetime. For example, immediately after stopping UV irradiation, the UPE lifetime is in the order of minutes (more than 5 min) [31]. Due to this difference in the emission lifetime, it is thought that the emission mechanism of UPE is different from that of fluorescence, and UPE spectra are also different from fluorescence spectra. Therefore, it is important to examine the unique spectral patterns of UVA-induced UPE.

Considering the emission wavelength of the excited species that cause UPE, the wavelengths of triplet-excited carbonyl are in the range of 350–550 nm [33]. It has been reported earlier that peak wavelength ranges of UPE spectra of biomolecules (DNA and amino acids, such as cysteine and tryptophan) oxidized by hydrogen peroxide and Fe^{2+} are within the wavelength range of triplet-excited carbonyl [84]. However, no such study has been performed for UVA irradiation. In the present study, the peak wavelength range of linoleic acid (450–490 nm) was close to the emission wavelength range of triplet excited carbonyl (350–550 nm), indicating that the triplet-excited carbonyls generated by UVA irradiation might contribute to the spectral pattern of linoleic acid.

UPE spectra for blood and collagen could not be obtained using the spectroscopy system in this study. For the blood sample, it is surmised that hemoglobin absorbed the generated UPE since hemoglobin is known to absorb light in the visible region [113],

thus matching the wavelength range of UVA-induced UPE. In chapter 3, there was no correlation between UPE intensity and the a* value reflecting cutaneous blood volume [139]; however, photon emission from the plasma in blood has been reported to have a UPE spectral range with a peak wavelength of 500–700 nm [140]. In this study, the plasma was not separated from the blood in order to confirm the UPE generation from whole blood. However, blood may indirectly be involved in UPE generation through energy transfer. Although collagen is known to be oxidized [141, 142], photon emission from UVA-irradiated collagen wasn't detected in this study. This result is consistent with the findings of a previous report [85], suggesting that the UVA-induced UPE wavelength of collagen is outside the detectable wavelength range as inferred from the fluorescence emission wavelength of collagen [87, 88, 132].

Based on the present findings and previous reports, some potential pathways for UVA-induced UPE generation in the skin are proposed (Figure 4.4). UVA directly causes UPE generation through the oxidation of biomolecules in the skin. Then, the UPE emission derived from the biomolecules is released from the skin surface. Conversely, it has been suggested that UPE is generated via a photosensitization reaction [86]. The chromophores in human skin act as photosensitizers and UVA induces the excited photosensitizers leading to ROS generation. Porphyrin [143] and melanin [144] in the

skin are known to cause photosensitization reactions, and other chromophores such as bilirubin, NADH, NADPH, *trans*-urocanic acid, and tryptophan have also been proposed as photosensitizers [145]. The study in chapter 3 showed a correlation of porphyrin with UPE. UVA excites photosensitizers in the skin, which in turn oxidize biomolecules, thus resulting in the release of UPE from the skin's surface. Moreover, the excited photosensitizer itself can act as an UPE source [33]. However, some biomolecules can receive energy from excited molecular species in the skin, and it is believed that photons of different wavelengths are emitted through energy transfer. In this way, a more complex mechanism of UPE generation and energy transfer may occur in the skin, suggesting that UPE is detected as an assembly of photons of various wavelengths. Although this study mainly focused on UVA-induced UPE, a separate mechanism may be operating with respect to UVB-induced UPE since there are chromophores that specifically absorb light in the UVB region [146].

Although a complex scheme is inferred (as shown in Figure 4.4), the results show that the UPE spectrum of phospholipids and the spectrum of skin tissue are similar. Hence, it is proposed that in UVA-exposed skin, phospholipid oxidation is a major contributor of UPE generation. The results in this study regarding phospholipids showed that the UPE generated came from the direct oxidation of the phospholipids by UVA irradiation.

However, ROS is generated in actual skin by a photosensitization reaction with UVA irradiation and it is thought that phospholipids are also oxidized by ROS. Phospholipids are the main components of the cell membrane [147], and therefore, it is important to understand the oxidative stress of phospholipids since their oxidation may have a considerable effect on cell function. However, since other biomolecules are also considered to be contributors to UPE generation from skin, the wavelengths of UPE emission for each biomolecule investigated in this study are expected to contribute toward elucidating the complicated mechanisms of UPE generation.

In this study there were some limitations that should be taken into consideration when evaluating the results. It is difficult to elucidate the mechanism underlying UPE generation in response to UVA irradiation from the obtained data. As the skin is made up of various components, it was not feasible to evaluate all the biomolecules. Therefore, the focus was on the major biomolecules known to oxidize in the skin. Herein, the mechanism of UPE was discussed with respect to the previously reported spectral analyses of biomolecules as well as the studies on UPE; however, further research involving other skin biomolecules is required. Nonetheless, it is believed that the data presented will contribute to the elucidation of the mechanisms involved in UPE generation. In addition, this study may provide insights into the diagnosis of skin

diseases induced by oxidative stress through the use of UPE measurement.

Figures and Tables

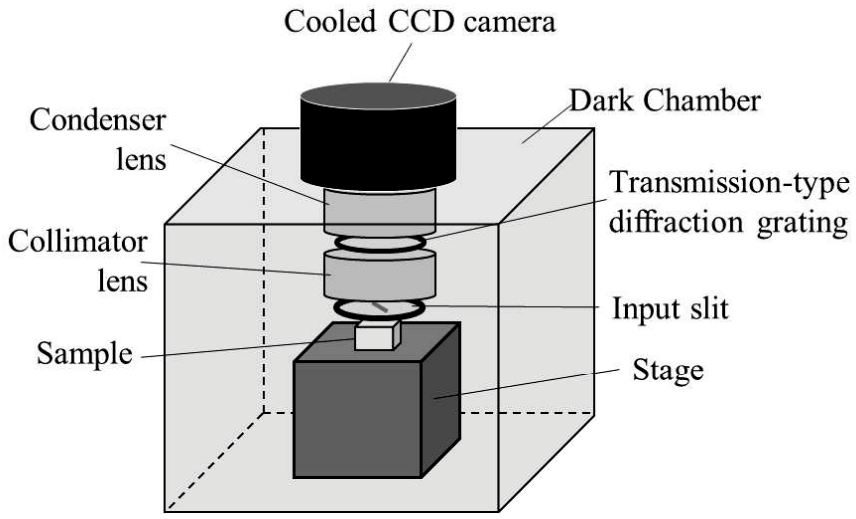

Figure 4.1. Schematic illustration of polychromatic spectroscopy

The UPE spectra of the samples were measured using a polychromatic spectrum analysis system, which consists of a transmission-type diffraction grating, condenser lens, collimator lens, input slit, and cooled CCD camera. The samples were irradiated with UVA outside of the dark chamber and were then immediately placed under a 1 mm wide and 20 mm high optical input slit in the dark chamber of the spectroscopic system.

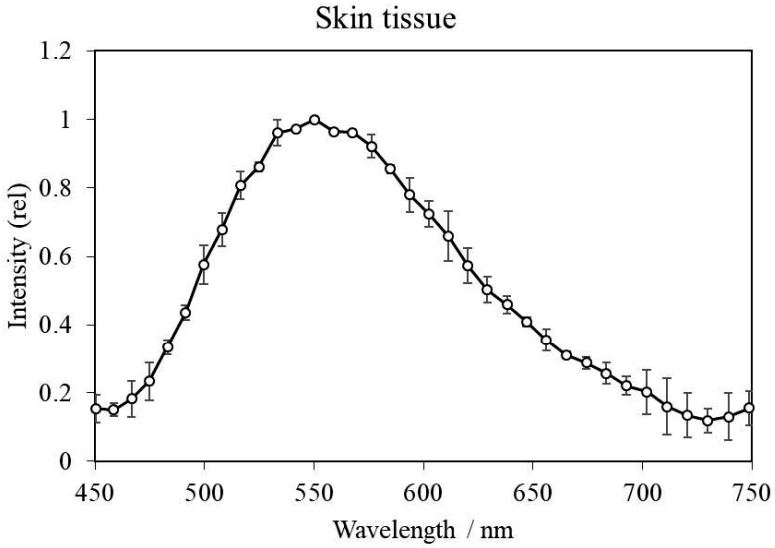

Figure 4.2. UVA-induced UPE spectrum of human skin tissue

Human skin tissue was irradiated with UVA and UPE spectra were measured using a spectroscopy system. The UPE intensity was normalized by the intensity at the peak wavelength and is displayed as relative intensity (rel). Data are presented as means ± SD (n = 3).

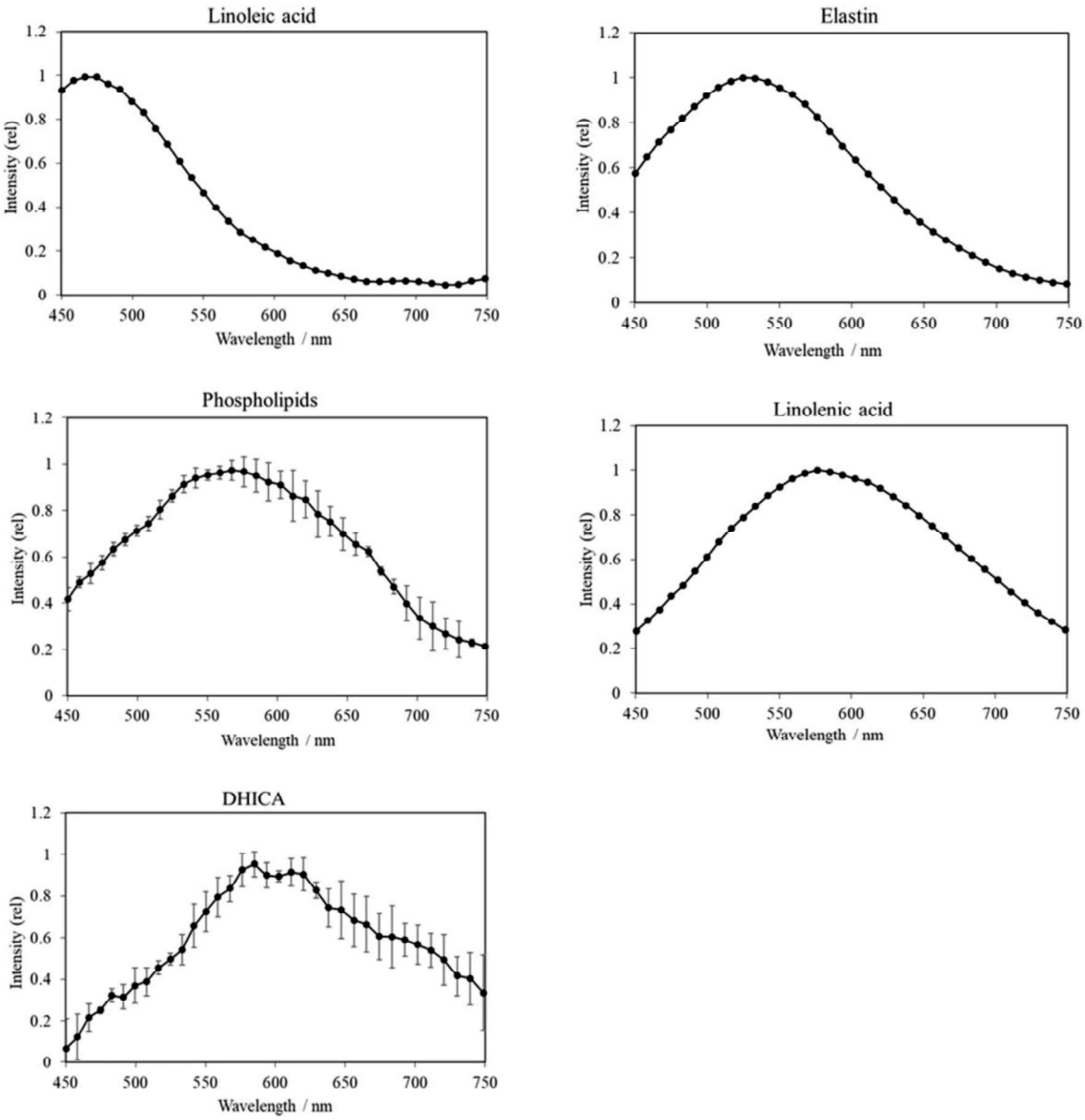

Figure 4.3. UVA-induced UPE spectra of biomolecules

Samples were irradiated with UVA and UPE spectra were measured using a spectroscopy system. UPE intensities were normalized by the intensity at the peak wavelength and are displayed as the relative intensity (rel). Data are presented as means ± SD (n = 4, phospholipids and DHICA). Spectra of raw materials were measured for all biomolecules except for DHICA, for which a 1 mM solution was used for measurement.

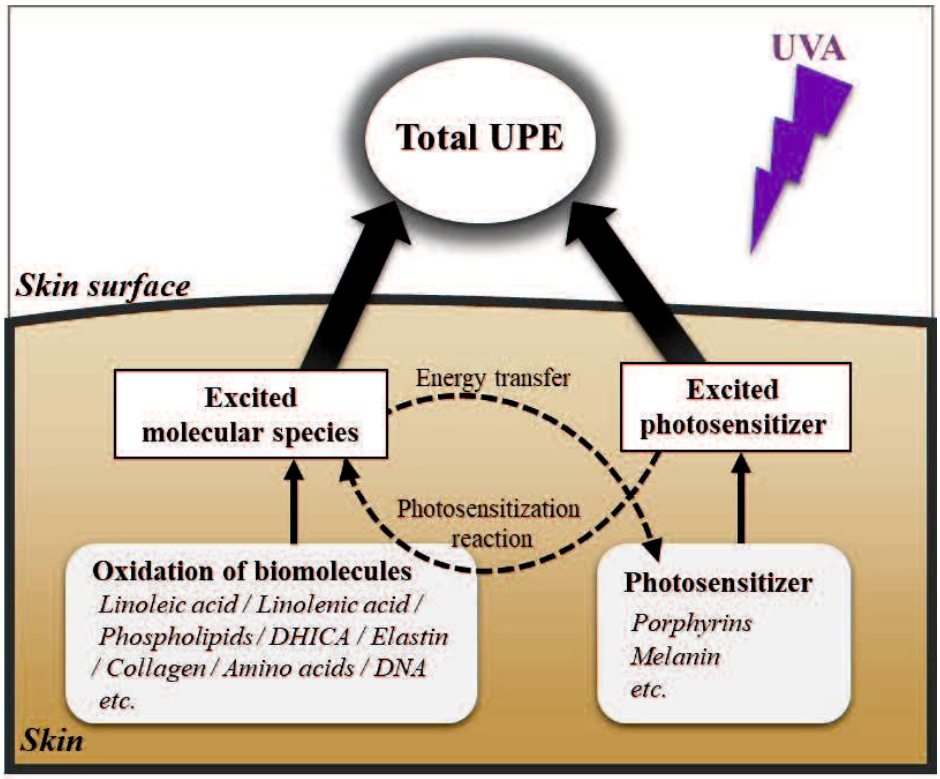

Figure 4.4. Scheme of proposed mechanism of UPE generation in skin by UVA irradiation

UVA irradiation causes UPE generation through oxidation of biomolecules in the skin via several pathways. Biomolecules exposed to UV directly generate UPE, while photosensitizers in the skin are excited by UV exposure. The excited photosensitizers oxidize biomolecules, and UPE is generated via the photosensitization reaction. The excited photosensitizer itself can act as a UPE source too. The UPE measured by the spectroscopy system, therefore, must have comprised the UPE from each of these pathways with a broad spectral pattern that peaked at 530–580 nm.

Table 4.1. Peak (relative intensity > 0.9) wavelength ranges of UVA-induced UPE spectra

Data are presented as means ± SD (n = 3 human skin tissue, n = 4 phospholipids and DHICA). UPE intensities at spectral peak are listed along with the peak wavelength (nm).

Emission source	Peak wavelength range (nm)	UPE intensity (counts/min) at peak wavelength
Human skin tissue	530 – 580	160 ± 11 [550 nm]
Linoleic acid	450 – 490	2760 [475 nm]
Elastin	500 – 560	10930 [525 nm]
Phospholipids	530 – 600	1230 ± 660 [570 nm]
Linolenic acid	550 – 620	5610 [575 nm]
DHICA	570 – 620	320 ± 95 [585 nm]

DHICA: 5,6-dihydroxyindole-2-carboxylic acid.

SUMMARY AND CONCLUSION

In humans and animals, the skin comes into contact with the outside and has the important functions of maintaining the body's homeostasis while also preventing the infiltration of external factors and the transpiration of water from the body. However, human skin is routinely exposed to ultraviolet (UV) rays and is subject to oxidative stress through the generation of reactive oxygen species (ROS). It is important to understand skin oxidative stress as it affects skin function and has been reported to be associated with skin diseases. On the other hand, it has long been known that ultraweak photon emission (UPE), also called the biophoton, is spontaneously generated from living organisms. Although the mechanism of its occurrence has not been clarified, it is known that UPE generates during the oxidation reaction, and it has been studied as a biological phenomenon which can be observed without the need for reagents.

Regarding these facts, chapter 2 verifies the usefulness of the evaluation method for skin oxidative stress using UPE measurement. Chapter 3 evaluates oxidative stress of facial skin by measuring the UPE and its relationship to skin properties. Furthermore, in chapter 4, spectrum analysis is used to elucidate the mechanisms of UPE generation in the skin.

In chapter 2, UV-induced UPE generating from skin tissue was imaged using a cooled CCD camera. The skin's UPE intensity is dependent on UV dose, and it is posited that

UPE may be generated not only from the epidermis but also the dermis. It was also found that UV-induced UPE can be suppressed by various antioxidants. UPE was positively found to be related to oxidation. Furthermore, the imaging method used in this experiment was able to visualize the UV-blocking effect of sunscreens. These results show that UPE measurement is useful for evaluating the oxidative stress of skin tissue as a whole.

Next, in chapter 3, the relationship between UPE intensity and skin properties on the entire human face was evaluated using the imaging method. As a result, it was shown that UPE intensity of the facial skin was non-uniform, indicating that oxidative stress differs depending on the facial part. It was suggested that the nose, which is reported to have a high incidence of skin cancer, has chronically high oxidative stress. In addition, UPE intensity in the skin around the eyes not only increases with age, but also shows a positive correlation with the wrinkle score, which is considered to reflect the skin properties of the face that are chronically exposed to UV. Although verification of the entire face can't be performed by conventional invasive methods, evaluating the oxidative stress of the face by applying UPE measurement was achieved in this study, and UPE intensity showed an important relationship with skin properties.

Finally, in chapter 4, in order to investigate the mechanism of UPE generation in the skin, polychromatic spectral analysis of UPE induced by UVA was performed. As a result,

the UPE generated from the skin tissue showed a broad spectral pattern with a peak at around 550 nm. In addition, the biomolecules contained in the human skin were similarly irradiated with UVA, and the spectra of UVA-induced UPE were measured. Various biomolecules showed spectra with peaks at different wavelengths, and in particular, phospholipids showed a spectrum pattern similar to that of UPE from skin tissue, suggesting that it contributes relatively significantly as a UPE source in skin. Since phospholipids are the main component of cell membranes, it is presumed that UVA-induced UPE also reflects the oxidative stress of cells. On the other hand, since UVA-induced UPE was not measured from blood, it is considered that UPE is absorbed by hemoglobin in the blood. Considering the photosensitization reaction in addition to the results obtained in this study, it is proposed that UPE generation from the skin has complicated mechanisms.

In conclusion, it was confirmed that UPE measurement is useful for evaluating the acute and chronic oxidative stress states of the skin. Also, the UPE mechanism in the skin was partially elucidated, demonstrating a relationship between the UPE of the skin and the skin's properties. Since mammalians have similar skin structures [148], it is assumed that a similar mechanism of UPE generation can be found in non-human mammals. UPE has been observed not only in humans but also in animals and it may be applicable to tumor

diagnosis for small animals and in follow-ups after radiotherapy. This UPE-measurement method can evaluate oxidative stress without contact or labeling, and with no significant burden on the living body. Therefore, it is expected that this non-invasive UPE diagnostic method will have a variety of applications in both human and veterinary medicine.

REFERENCES

1. Kobayashi, M., Kikuchi, D. & Okamura, H. Imaging of ultraweak spontaneous photon emission from human body displaying diurnal rhythm. *PLoS One* **4**, e6256 (2009).

2. Shimizu, H. *Textbook of Modern Dermatology 3rd edition*. 1–35 (Nakayama Shoten, 2018).

3. Jablonski, N. G. & Chaplin, G. Human skin pigmentation as an adaptation to UV radiation. *Proc. Natl. Acad. Sci. U. S. A.* **107**, 8962-8968 (2010).

4. Diffey, B. L. Sources and measurement of ultraviolet radiation. *Methods* **28**, 4-13 (2002).

5. Fisher, G. J., Kang, S., Varani, J., Bata-Csorgo, Z., Wan, Y., Datta, S. & Voorhees, J. J. Mechanisms of photoaging and chronological skin aging. *Arch. Dermatol.* **138**, 1462-1470 (2002).

6. Fisher, G. J., Wang, Z. Q., Datta, S. C., Varani, J., Kang, S. & Voorhees, J. J. Pathophysiology of premature skin aging induced by ultraviolet light. *N. Engl. J. Med.* **337**, 1419-1428 (1997).

7. Routaboul, C., Denis, A. & Vinche, A. Immediate pigment darkening: description, kinetic and biological function. *Eur. J. Dermatol.* **9**, 95-99 (1999).

8. Yasui, H. & Sakurai, H. Chemiluminescent detection and imaging of reactive oxygen species in live mouse skin exposed to UVA. *Biochem. Biophys. Res. Commun.* **269**, 131-136 (2000).

9. Shono, S., Imura, M., Ota, M., Ono, S. & Toda, K. The relationship of skin color, UVB-induced erythema, and melanogenesis. *J. Invest. Dermatol.* **84**, 265-267 (1985).

10. Piotrowska, A., Wierzbicka, J. & Żmijewski, M. A. Vitamin D in the skin physiology and pathology. *Acta Biochim. Pol.* **63**, 17-29 (2016).

11. Taylor, C. R., Stern, R. S., Leyden, J. J. & Gilchrest, B. A. Photoaging/photodamage and photoprotection. *J. Am. Acad. Dermatol.* **22**, 1-15 (1990).

12. Fisher, G. J., Datta, S. C., Talwar, H. S., Wang, Z. Q., Varani, J., Kang, S. & Voorhees, J. J. Molecular basis of sun-induced premature skin ageing and retinoid antagonism. *Nature* **379**, 335-339 (1996).

13. Thiers, B. H., Maize, J. C., Spicer, S. S. & Cantor, A. B. The effect of aging and chronic sun exposure on human Langerhans cell populations. *J. Invest. Dermatol.* **82**, 223-226 (1984).

14. Leiter, U., Keim, U. & Garbe, C. Epidemiology of Skin Cancer: Update 2019. *Adv.*

Exp. Med. Biol. **1268**, 123-139 (2020).

15. de Gruijl, F. R. Skin cancer and solar UV radiation. *Eur. J. Cancer* **35**, 2003-2009 (1999).

16. Forman, H. J., Maiorino, M. & Ursini, F. Signaling functions of reactive oxygen species. *Biochemistry* **49**, 835-842 (2010).

17. Venditti, P. & Di Meo, S. The Role of Reactive Oxygen Species in the Life Cycle of the Mitochondrion. *Int. J. Mol. Sci.* **21**, 2173 (2020).

18. Xian, D., Lai, R., Song, J., Xiong, X. & Zhong, J. Emerging Perspective: Role of Increased ROS and Redox Imbalance in Skin Carcinogenesis. *Oxid. Med. Cell. Longev.* **2019**, 8127362 (2019).

19. Singh, A. Chemical and biochemical aspects of superoxide radicals and related species of activated oxygen. *Can. J. Physiol. Pharmacol.* **60**, 1330-1345 (1982).

20. Rinnerthaler, M., Bischof, J., Streubel, M. K., Trost, A. & Richter, K. Oxidative stress in aging human skin. *Biomolecules* **5**, 545-589 (2015).

21. Okayama, Y. Oxidative stress in allergic and inflammatory skin diseases. *Curr. Drug Targets Inflamm. Allergy* **4**, 517-519 (2005).

22. Briganti, S. & Picardo, M. Antioxidant activity, lipid peroxidation and skin diseases. What's new. *J. Eur. Acad. Dermatol. Venereol.* **17**, 663-669 (2003).

23. Kruk, J. & Duchnik, E. Oxidative stress and skin diseases: possible role of physical activity. *Asian Pac. J. Cancer Prev.* **15**, 561-568 (2014).

24. Kapun, A. P., Salobir, J., Levart, A., Kotnik, T. & Svete, A. N. Oxidative stress markers in canine atopic dermatitis. *Res. Vet. Sci.* **92**, 469-470 (2012).

25. Almela, R. M., Rubio, C. P., Cerón, J. J., Ansón, A., Tichy, A. & Mayer, U. Selected serum oxidative stress biomarkers in dogs with non-food-induced and food-induced atopic dermatitis. *Vet. Dermatol.* **29**, 229-e282 (2018).

26. Ping, Z., Peng, Y., Lang, H., Xinyong, C., Zhiyi, Z., Xiaocheng, W., Hong, Z. & Liang, S. Oxidative Stress in Radiation-Induced Cardiotoxicity. *Oxid. Med. Cell. Longev.* **2020**, 3579143 (2020).

27. Nomiya, T., Kaneko, T., Goto, J., Harada, M., Akamatsu, H., Hagiwara, Y., Ota, I. & Nemoto, K. Relationship between serum reactive oxidative metabolite level and skin reaction in an irradiated rat model. *Free Radic. Res.* **48**, 572-579 (2014).

28. Kopáni, M., Celec, P., Danisovic, L., Michalka, P. & Biró, C. Oxidative stress and electron spin resonance. *Clin. Chim. Acta* **364**, 61-66 (2006).

29. Murtas, D., Piras, F., Minerba, L., Ugalde, J., Floris, C., Maxia, C., Demurtas, P., Perra, M. T. & Sirigu, P. Nuclear 8-hydroxy-2'-deoxyguanosine as survival biomarker in patients with cutaneous melanoma. *Oncol. Rep.* **23**, 329-335 (2010).

30. Rhie, G., Shin, M. H., Seo, J. Y., Choi, W. W., Cho, K. H., Kim, K. H., Park, K. C., Eun, H. C. & Chung, J. H. Aging- and photoaging-dependent changes of enzymic and nonenzymic antioxidants in the epidermis and dermis of human skin in vivo. *J. Invest. Dermatol.* **117**, 1212-1217 (2001).

31. Ou-Yang, H., Stamatas, G., Saliou, C. & Kollias, N. A chemiluminescence study of UVA-induced oxidative stress in human skin in vivo. *J. Invest. Dermatol.* **122**, 1020-1029 (2004).

32. Havaux, M., Triantaphylidès, C. & Genty, B. Autoluminescence imaging: a non-invasive tool for mapping oxidative stress. *Trends Plant Sci* **11**, 480-484 (2006).

33. Pospíšil, P., Prasad, A. & Rác, M. Role of reactive oxygen species in ultra-weak photon emission in biological systems. *J. Photochem. Photobiol. B* **139**, 11-23 (2014).

34. Kobayashi, K., Okabe, H., Kawano, S., Hidaka, Y. & Hara, K. Biophoton emission induced by heat shock. *PLoS One* **9**, e105700 (2014).

35. Ou-Yang, H. The application of ultra-weak photon emission in dermatology. *J. Photochem. Photobiol. B* **139**, 63-70 (2014).

36. Takeda, M., Kobayashi, M., Takayama, M., Suzuki, S., Ishida, T., Ohnuki, K., Moriya, T. & Ohuchi, N. Biophoton detection as a novel technique for cancer

imaging. *Cancer Sci.* **95**, 656-661 (2004).

37. Van Wijk, R., Kobayashi, M. & Van Wijk, E. P. Anatomic characterization of human ultra-weak photon emission with a moveable photomultiplier and CCD imaging. *J. Photochem. Photobiol. B* **83**, 69-76 (2006).

38. Gurwitsch, A. G., Grabje, S. & Salkind, S. Die Natur des spezifischen Erregers der Zellteilung. *Arch. Entw. Mech.* **100**, 11-40 (1923).

39. Gurwitsch, A. A. A historical review of the problem of mitogenetic radiation. *Experientia* **44**, 545-550 (1988).

40. Gurwitsch, A. & Gurwitsch, L. Ultra-Violet Chemi-Luminescence. *Nature* **143**, 1022-1023 (1939).

41. Abeles, F. B. Plant chemiluminescence. *Annu Rev Plant Physiol* **37**, 49-72 (1986).

42. Colli, L., Facchini, U., Guidotti, G., Dugnani Lonati, R., Orsenigo, M. & Sommariva, O. Further measurements on the bioluminescence of the seedlings. *Experientia* **11**, 479-481 (1955).

43. Konev, S. V., Lyskova, T. I. & Nisenbaum, G. D. On the problem of the very faint bioluminescence of cells in the ultraviolet range of the spectrum and its biological role. *Biofizika* **11**, 361-363 (1966).

44. Popov, G. A. & Tarusov, B. N. On the nature of the spontaneous luminescence of

animal tissues. *Biofizika* **8**, 317-320 (1963).

45. Zhuravlev, A. I., Tsvylev, O. P. & Zubkova, S. M. Spontaneous endogenous ultraweak luminescence of rat liver mitochondria in conditions of normal metabolism. *Biofizika* **18**, 1037-1040 (1973).

46. Quickenden, T. I. & Que Hee, S. S. The spectral distribution of the luminescence emitted during growth of the yeast Saccharomyces cerevisiae and its relationship to mitogenetic radiation. *Photochem. Photobiol.* **23**, 201-204 (1976).

47. Shimizu, Y., Inaba, H., Kumaki, K., Mizuno, K., Hata, S. & Tomioka, S. Measuring methods for ultra-low light intensity and their application to extra-weak spontaneous bioluminescence from living tissues. *IEEE Trans Instrum Meas* **22**, 153-157 (1973).

48. Inaba, H., Shimizu, Y., Tsuji, Y. & Yamacishi, A. Photon counting spectral analyzing system of extra-weak chemi- and bioluminescence for biochemical applications. *Photochem. Photobiol.* **30**, 169-175 (1979).

49. Inaba, H., Yamagishi, A., Takyu, C., Yoda, B., Goto, Y., Miyazawa, T., Kaneda, T. & Saeki, A. Development of an ultra-high sensitive photon counting system and its application to biomedical measurements. *Opt Lasers Eng* **3**, 125-130 (1982).

50. Scott, R. Q., Usa, M. & Inaba, H. Ultraweak emission imagery of mitosing

soybeans. *Appl Phys B* **48**, 183-185 (1989).

51. Suzuki, S., Usa, M., Nagoshi, T., Kobayashi, M., Watanabe, N., Watanabe, H. & Inaba, H. Two-dimensional imaging and counting of ultraweak emission patterns from injured plant seedlings. *J. Photochem. Photobiol. B* **9**, 211-217 (1991).

52. Devaraj, B., Usa, M. & Inaba, H. Biophotons: ultraweak light emission from living systems. *Curr Opin Solid State Mater Sci* **2**, 188-193 (1997).

53. Scholz, W., Staszkiewicz, U., Popp, F. A. & Nagl, W. Light-stimulated ultraweak photon reemission of human amnion cells and Wish cells. *Cell Biophys.* **13**, 55-63 (1988).

54. Hideg, E. & Inaba, H. Biophoton emission (ultraweak photoemission) from dark adapted spinach chloroplasts. *Photochem. Photobiol.* **53**, 137-142 (1991).

55. Panagopoulos, I., Bornman, J. F. & Björn, L. O. Effects of ultraviolet radiation and visible light on growth, fluorescence induction, ultraweak luminescence and peroxidase activity in sugar beet plants. *J Photochem Photobiol B* **8**, 73-87 (1990).

56. van Wijk, R. & van Aken, H. Light-induced photon emission by rat hepatocytes and hepatoma cells. *Cell Biophys.* **18**, 15-29 (1991).

57. Grasso, F., Grillo, C., Musumeci, F., Triglia, A., Rodolico, G., Cammisuli, F., Rinzivillo, C., Fragati, G., Santuccio, A. & Rodolico, M. Photon emission from

normal and tumor human tissues. *Experientia* **48**, 10-13 (1992).

58. Kobayashi, M. Two-dimensional imaging and spatiotemporal analysis of biophoton. *Biophotonics*, 155-171 (2005).

59. Usui, S., Tada, M. & Kobayashi, M. Non-invasive visualization of physiological changes of insects during metamorphosis based on biophoton emission imaging. *Sci. Rep.* **9**, 8576 (2019).

60. Niggli, H. J. Ultraweak photons emitted by cells: biophotons. *J. Photochem. Photobiol. B* **14**, 144-146 (1992).

61. de Mello Gallep, C. Ultraweak, spontaneous photon emission in seedlings: toxicological and chronobiological applications. *Luminescence* **29**, 963-968 (2014).

62. Zapata, F., Pastor-Ruiz, V., Ortega-Ojeda, F., Montalvo, G., Ruiz-Zolle, A. V. & García-Ruiz, C. Human ultra-weak photon emission as non-invasive spectroscopic tool for diagnosis of internal states - A review. *J. Photochem. Photobiol. B* **216**, 112141 (2021).

63. Prasad, A. & Pospíšil, P. Towards the two-dimensional imaging of spontaneous ultra-weak photon emission from microbial, plant and animal cells. *Sci. Rep.* **3**, 1211 (2013).

64. Nakamura, K. & Hiramatsu, M. Ultra-weak photon emission from human hand: influence of temperature and oxygen concentration on emission. *J. Photochem. Photobiol. B* **80**, 156-160 (2005).

65. Hagens, R., Khabiri, F., Schreiner, V., Wenck, H., Wittern, K. P., Duchstein, H. J. & Mei, W. Non-invasive monitoring of oxidative skin stress by ultraweak photon emission measurement. II: biological validation on ultraviolet A-stressed skin. *Skin Res. Technol.* **14**, 112-120 (2008).

66. Sauermann, G., Mei, W. P., Hoppe, U. & Stäb, F. Ultraweak photon emission of human skin in vivo: influence of topically applied antioxidants on human skin. *Methods Enzymol.* **300**, 419-428 (1999).

67. Miyamoto, S., Ronsein, G. E., Prado, F. M., Uemi, M., Corrêa, T. C., Toma, I. N., Bertolucci, A., Oliveira, M. C., Motta, F. D., Medeiros, M. H. & Mascio, P. D. Biological hydroperoxides and singlet molecular oxygen generation. *IUBMB Life* **59**, 322-331 (2007).

68. Inaba, H. & Shimizu, Y. *Study on Information About Living System by Biophoton*. (Tohoku University Press, Sendai, 2011).

69. Kobayashi, M. Highly sensitive imaging for ultra-weak photon emission from living organisms. *J. Photochem. Photobiol. B* **139**, 34-38 (2014).

70. Bickers, D. R. & Athar, M. Oxidative stress in the pathogenesis of skin disease. *J. Invest. Dermatol.* **126**, 2565-2575 (2006).

71. Svobodova, A., Walterova, D. & Vostalova, J. Ultraviolet light induced alteration to the skin. *Biomed. Pap. Med. Fac. Univ. Palacky Olomouc Czech. Repub.* **150**, 25-38 (2006).

72. Rittié, L. & Fisher, G. J. UV-light-induced signal cascades and skin aging. *Ageing Res Rev* **1**, 705-720 (2002).

73. Ekanayake Mudiyanselage, S., Hamburger, M., Elsner, P. & Thiele, J. J. Ultraviolet a induces generation of squalene monohydroperoxide isomers in human sebum and skin surface lipids in vitro and in vivo. *J. Invest. Dermatol.* **120**, 915-922 (2003).

74. Fujita, H., Hirao, T. & Takahashi, M. A simple and non-invasive visualization for assessment of carbonylated protein in the stratum corneum. *Skin Res. Technol.* **13**, 84-90 (2007).

75. Sander, C. S., Chang, H., Salzmann, S., Müller, C. S., Ekanayake-Mudiyanselage, S., Elsner, P. & Thiele, J. J. Photoaging is associated with protein oxidation in human skin in vivo. *J. Invest. Dermatol.* **118**, 618-625 (2002).

76. Kobayashi, M., Iwasa, T. & Tada, M. Polychromatic spectral pattern analysis of

ultra-weak photon emissions from a human body. *J. Photochem. Photobiol. B* **159**, 186-190 (2016).

77. Nozawa, H., Yamamoto, H., Makita, K., Schuch, N. J., Pinhiero, D. K., Carbone, S., Mac-Mahon, R. M. & Foppiano, A. J. Ground-based observation of solar UV radiation in Japan, Brazil and Chile. *Rev. Bras. Geof* **25**, 17-25 (2007).

78. INTERNATIONAL PROGRAMME ON CHEMICAL SAFETY, Environmental health criteria 160, ultraviolet radiation. (1994). <http://www.inchem.org/documents/ehc/ehc/ehc160.htm>.

79. Bruls, W. A., Slaper, H., van der Leun, J. C. & Berrens, L. Transmission of human epidermis and stratum corneum as a function of thickness in the ultraviolet and visible wavelengths. *Photochem. Photobiol.* **40**, 485-494 (1984).

80. Evelson, P., Ordóñez, C. P., Llesuy, S. & Boveris, A. Oxidative stress and in vivo chemiluminescence in mouse skin exposed to UVA radiation. *J. Photochem. Photobiol. B* **38**, 215-219 (1997).

81. Rastogi, A. & Pospísil, P. Spontaneous ultraweak photon emission imaging of oxidative metabolic processes in human skin: effect of molecular oxygen and antioxidant defense system. *J. Biomed. Opt.* **16**, 096005 (2011).

82. Egawa, M., Kohno, Y. & Kumano, Y. Oxidative effects of cigarette smoke on the

human skin. *Int. J. Cosmet. Sci.* **21**, 83-98 (1999).

83. Prasad, A. & Pospišil, P. Two-dimensional imaging of spontaneous ultra-weak photon emission from the human skin: role of reactive oxygen species. *J Biophotonics* **4**, 840-849 (2011).

84. Khabiri, F., Hagens, R., Smuda, C., Soltau, A., Schreiner, V., Wenck, H., Wittern, K. P., Duchstein, H. J. & Mei, W. Non-invasive monitoring of oxidative skin stress by ultraweak photon emission (UPE)-measurement. I: mechanisms of UPE of biological materials. *Skin Res. Technol.* **14**, 103-111 (2008).

85. Ou-Yang, H., Stamatas, G. & Kollias, N. Dermal contributions to UVA-induced oxidative stress in skin. *Photodermatol. Photoimmunol. Photomed.* **25**, 65-70 (2009).

86. Prasad, A. & Pospíšil, P. Ultraweak photon emission induced by visible light and ultraviolet A radiation via photoactivated skin chromophores: in vivo charge coupled device imaging. *J. Biomed. Opt.* **17**, 085004 (2012).

87. Gillies, R., Zonios, G., Anderson, R. R. & Kollias, N. Fluorescence excitation spectroscopy provides information about human skin in vivo. *J. Invest. Dermatol.* **115**, 704-707 (2000).

88. Laiho, L. H., Pelet, S., Hancewicz, T. M., Kaplan, P. D. & So, P. T. Two-photon

3-D mapping of ex vivo human skin endogenous fluorescence species based on fluorescence emission spectra. *J. Biomed. Opt.* **10**, 024016 (2005).

89. Sakura, S., Fujimoto, D., Sakamoto, K., Mizuno, A. & Motegi, K. Photolysis of pyridinoline, a cross-linking amino acid of collagen, by ultraviolet light. *Can. J. Biochem.* **60**, 525-529 (1982).

90. Sander, C. S., Hamm, F., Elsner, P. & Thiele, J. J. Oxidative stress in malignant melanoma and non-melanoma skin cancer. *Br. J. Dermatol.* **148**, 913-922 (2003).

91. Sabharwal, S. S. & Schumacker, P. T. Mitochondrial ROS in cancer: initiators, amplifiers or an Achilles' heel? *Nat. Rev. Cancer* **14**, 709-721 (2014).

92. Li, J. M. & Shah, A. M. ROS generation by nonphagocytic NADPH oxidase: potential relevance in diabetic nephropathy. *J. Am. Soc. Nephrol.* **14**, S221-226 (2003).

93. Uchino, T., Tokunaga, H., Onodera, H. & Ando, M. Effect of squalene monohydroperoxide on cytotoxicity and cytokine release in a three-dimensional human skin model and human epidermal keratinocytes. *Biol. Pharm. Bull.* **25**, 605-610 (2002).

94. Genov, M., Kreiseder, B., Nagl, M., Drucker, E., Wiederstein, M., Muellauer, B., Krebs, J., Grohmann, T., Pretsch, D., Baumann, K., Bacher, M., Pretsch, A. &

Wiesner, C. Tetrahydroanthraquinone Derivative (±)-4-Deoxyaustrocortilutein Induces Cell Cycle Arrest and Apoptosis in Melanoma Cells via Upregulation of p21 and p53 and Downregulation of NF-kappaB. *J. Cancer* **7**, 555-568 (2016).

95. Berneburg, M., Plettenberg, H. & Krutmann, J. Photoaging of human skin. *Photodermatol. Photoimmunol. Photomed.* **16**, 239-244 (2000).

96. Wa, C. V. & Maibach, H. I. Mapping the human face: biophysical properties. *Skin Res. Technol.* **16**, 38-54 (2010).

97. Marrakchi, S. & Maibach, H. I. Biophysical parameters of skin: map of human face, regional, and age-related differences. *Contact Dermatitis* **57**, 28-34 (2007).

98. Akiba, S., Shinkura, R., Miyamoto, K., Hillebrand, G., Yamaguchi, N. & Ichihashi, M. Influence of chronic UV exposure and lifestyle on facial skin photo-aging--results from a pilot study. *J. Epidemiol.* **9**, S136-142 (1999).

99. Yin, Y., Li, J., Li, Q., Zhang, A. & Jin, P. Autologous fat graft assisted by stromal vascular fraction improves facial skin quality: A randomized controlled trial. *J. Plast. Reconstr. Aesthet. Surg.* **73**, 1166-1173 (2020).

100. Kim, B. R., Chun, M. Y., Kim, S. A. & Youn, S. W. Sebum Secretion of the Trunk and the Development of Truncal Acne in Women: Do Truncal Acne and Sebum Affect Each Other? *Dermatology* **231**, 87-93 (2015).

101. Lopez, S., Le Fur, I., Morizot, F., Heuvin, G., Guinot, C. & Tschachler, E. Transepidermal water loss, temperature and sebum levels on women's facial skin follow characteristic patterns. *Skin Res. Technol.* **6**, 31-36 (2000).

102. Vuyk, H. D. & Lohuis, P. J. Mohs micrographic surgery for facial skin cancer. *Clin. Otolaryngol. Allied Sci.* **26**, 265-273 (2001).

103. Buettner, P. G. & Raasch, B. A. Incidence rates of skin cancer in Townsville, Australia. *Int. J. Cancer* **78**, 587-593 (1998).

104. Sander, C. S., Chang, H., Hamm, F., Elsner, P. & Thiele, J. J. Role of oxidative stress and the antioxidant network in cutaneous carcinogenesis. *Int. J. Dermatol.* **43**, 326-335 (2004).

105. Toyokuni, S. Novel aspects of oxidative stress-associated carcinogenesis. *Antioxid Redox Signal* **8**, 1373-1377 (2006).

106. Chopra, K., Calva, D., Sosin, M., Tadisina, K. K., Banda, A., De La Cruz, C., Chaudhry, M. R., Legesse, T., Drachenberg, C. B., Manson, P. N. & Christy, M. R. A comprehensive examination of topographic thickness of skin in the human face. *Aesthet. Surg. J.* **35**, 1007-1013 (2015).

107. Kammeyer, A. & Luiten, R. M. Oxidation events and skin aging. *Ageing Res Rev* **21**, 16-29 (2015).

108. Shin, M. H., Seo, J. E., Kim, Y. K., Kim, K. H. & Chung, J. H. Chronic heat treatment causes skin wrinkle formation and oxidative damage in hairless mice. *Mech. Ageing Dev.* **133**, 92-98 (2012).

109. Chiba, K., Sone, T., Kawakami, K. & Onoue, M. Skin roughness and wrinkle formation induced by repeated application of squalene-monohydroperoxide to the hairless mouse. *Exp. Dermatol.* **8**, 471-479 (1999).

110. Asawanonda, P. & Taylor, C. R. Wood's light in dermatology. *Int. J. Dermatol.* **38**, 801-807 (1999).

111. Maitra, D., Bragazzi Cunha, J., Elenbaas, J. S., Bonkovsky, H. L., Shavit, J. A. & Omary, M. B. Porphyrin-Induced Protein Oxidation and Aggregation as a Mechanism of Porphyria-Associated Cell Injury. *Cell. Mol. Gastroenterol. Hepatol.* **8**, 535-548 (2019).

112. Nishigori, C., Hattori, Y., Arima, Y. & Miyachi, Y. Photoaging and oxidative stress. *Exp. Dermatol.* **12 Suppl 2**, 18-21 (2003).

113. Patterson, M. S., Wilson, B. C. & Wyman, D. R. The propagation of optical radiation in tissue. II: Optical properties of tissues and resulting fluence distributions. *Lasers Med. Sci.* **6**, 379–390 (1991).

114. Ye, Z. W., Zhang, J., Townsend, D. M. & Tew, K. D. Oxidative stress, redox

regulation and diseases of cellular differentiation. *Biochim. Biophys. Acta* **1850**, 1607-1621 (2015).

115. Bartosz, G. Oxidative stress in plants. *Acta Physiologiae Plantarum* **19**, 47–64 (1997).

116. Lykkesfeldt, J. & Svendsen, O. Oxidants and antioxidants in disease: oxidative stress in farm animals. *Vet. J.* **173**, 502-511 (2007).

117. Tönnies, E. & Trushina, E. Oxidative Stress, Synaptic Dysfunction, and Alzheimer's Disease. *J. Alzheimers Dis.* **57**, 1105-1121 (2017).

118. Miyachi, Y. Photoaging from an oxidative standpoint. *J. Dermatol. Sci.* **9**, 79-86 (1995).

119. Nishigori, C., Hattori, Y. & Toyokuni, S. Role of reactive oxygen species in skin carcinogenesis. *Antioxid Redox Signal* **6**, 561-570 (2004).

120. Liu-Smith, F., Jia, J. & Zheng, Y. UV-Induced Molecular Signaling Differences in Melanoma and Non-melanoma Skin Cancer. *Adv. Exp. Med. Biol.* **996**, 27-40 (2017).

121. Wolf, A. M., Nishimaki, K., Kamimura, N. & Ohta, S. Real-time monitoring of oxidative stress in live mouse skin. *J. Invest. Dermatol.* **134**, 1701-1709 (2014).

122. Miyamoto, S., Martinez, G. R., Medeiros, M. H. & Di Mascio, P. Singlet

molecular oxygen generated by biological hydroperoxides. *J. Photochem. Photobiol. B* **139**, 24-33 (2014).

123. Van Wijk, E. P., Van Wijk, R. & Bosman, S. Using ultra-weak photon emission to determine the effect of oligomeric proanthocyanidins on oxidative stress of human skin. *J. Photochem. Photobiol. B* **98**, 199-206 (2010).

124. Prasad, A., Gouripeddi, P., Devireddy, H. R. N., Ovsii, A., Rachakonda, D. P., Wijk, R. V. & Pospíšil, P. Spectral Distribution of Ultra-Weak Photon Emission as a Response to Wounding in Plants: An In Vivo Study. *Biology (Basel)* **9**, 139 (2020).

125. Zhao, X., Yang, M., Wang, Y., Pang, J., Wijk, E. V., Liu, Y., Fan, H., Zhang, L. & Han, J. Spectrum of spontaneous photon emission as a promising biophysical indicator for breast cancer research. *Sci. Rep.* **7**, 13083 (2017).

126. Kubow, S. Routes of formation and toxic consequences of lipid oxidation products in foods. *Free Radic. Biol. Med.* **12**, 63-81 (1992).

127. Sasaguri, Y., Kakita, N., Murahashi, N., Kato, S., Hiraoka, K., Morimatsu, M. & Yagi, K. Effect of linoleic acid hydroperoxide on production of matrix metalloproteinases by human aortic endothelial and smooth muscle cells. *Atherosclerosis* **100**, 189-196 (1993).

128. Ohuchida, M., Sasaguri, Y., Morimatsu, M., Nagase, H. & Yagi, K. Effect of linoleic acid hydroperoxide on production of matrix metalloproteinases by human skin fibroblasts. *Biochem. Int.* **25**, 447-452 (1991).

129. Yin, L., Morita, A. & Tsuji, T. Skin aging induced by ultraviolet exposure and tobacco smoking: evidence from epidemiological and molecular studies. *Photodermatol. Photoimmunol. Photomed.* **17**, 178-183 (2001).

130. Sinclair, A. J., Attar-Bashi, N. M. & Li, D. What is the role of alpha-linolenic acid for mammals? *Lipids* **37**, 1113-1123 (2002).

131. Arantes, E. L., Dragano, N., Ramalho, A., Vitorino, D., de-Souza, G. F., Lima, M. H., Velloso, L. A. & Araújo, E. P. Topical Docosahexaenoic Acid (DHA) Accelerates Skin Wound Healing in Rats and Activates GPR120. *Biol. Res. Nurs.* **18**, 411-419 (2016).

132. Bottiroli, G. & Croce, A. C. Autofluorescence spectroscopy of cells and tissues as a tool for biomedical diagnosis. *Photochem Photobiol Sci* **3**, 189-210 (2004).

133. Wondrak, G. T., Roberts, M. J., Cervantes-Laurean, D., Jacobson, M. K. & Jacobson, E. L. Proteins of the extracellular matrix are sensitizers of photo-oxidative stress in human skin cells. *J. Invest. Dermatol.* **121**, 578-586 (2003).

134. Mythravaruni, P. & Ravindran, P. The effect of oxidation on the mechanical

response of isolated elastin and aorta. *J. Biomech. Eng.* **141**, 061002 (2019).

135. Bochkov, V. N., Oskolkova, O. V., Birukov, K. G., Levonen, A. L., Binder, C. J. & Stöckl, J. Generation and biological activities of oxidized phospholipids. *Antioxid Redox Signal* **12**, 1009-1059 (2010).

136. Kobayashi, T., Urabe, K., Winder, A., Jiménez-Cervantes, C., Imokawa, G., Brewington, T., Solano, F., García-Borrón, J. C. & Hearing, V. J. Tyrosinase related protein 1 (TRP1) functions as a DHICA oxidase in melanin biosynthesis. *EMBO J.* **13**, 5818-5825 (1994).

137. Pellosi, M. C., Suzukawa, A. A., Scalfo, A. C., Di Mascio, P., Martins Pereira, C. P., de Souza Pinto, N. C., de Luna Martins, D. & Martinez, G. R. Effects of the melanin precursor 5,6-dihydroxy-indole-2-carboxylic acid (DHICA) on DNA damage and repair in the presence of reactive oxygen species. *Arch. Biochem. Biophys.* **557**, 55-64 (2014).

138. Berezin, M. Y. & Achilefu, S. Fluorescence lifetime measurements and biological imaging. *Chem. Rev.* **110**, 2641-2684 (2010).

139. Takiwaki, H. Measurement of skin color: practical application and theoretical considerations. *J. Med. Invest.* **44**, 121-126 (1998).

140. Kobayashi, M., Usa, M. & Inaba, H. Highly sensitive detection and spectral

analysis of ultraweak photon emission from living samples of human origin for the measurement of biomedical information. *Trans Soc Instrum Control Eng* **30**, 385-391 (1994).

141. Kato, Y., Uchida, K. & Kawakishi, S. Oxidative degradation of collagen and its model peptide by ultraviolet irradiation. *J. Agric. Food Chem.* **40**, 373-379 (1992).

142. Bochi, G. V., Torbitz, V. D., de Campos, L. P., Sangoi, M. B., Fernandes, N. F., Gomes, P., Moretto, M. B., Barbisan, F., da Cruz, I. B. & Moresco, R. N. In Vitro Oxidation of Collagen Promotes the Formation of Advanced Oxidation Protein Products and the Activation of Human Neutrophils. *Inflammation* **39**, 916-927 (2016).

143. Granville, D. J. & Hunt, D. W. Porphyrin-mediated photosensitization - taking the apoptosis fast lane. *Curr Opin Drug Discov Devel* **3**, 232-243 (2000).

144. Takeuchi, S., Zhang, W., Wakamatsu, K., Ito, S., Hearing, V. J., Kraemer, K. H. & Brash, D. E. Melanin acts as a potent UVB photosensitizer to cause an atypical mode of cell death in murine skin. *Proc. Natl. Acad. Sci. U. S. A.* **101**, 15076-15081 (2004).

145. Wondrak, G. T., Jacobson, M. K. & Jacobson, E. L. Endogenous UVA-photosensitizers: mediators of skin photodamage and novel targets for skin

photoprotection. *Photochem Photobiol Sci* **5**, 215-237 (2006).

146. Young, A. R. Chromophores in human skin. *Phys. Med. Biol.* **42**, 789-802 (1997).

147. Ohvo-Rekilä, H., Ramstedt, B., Leppimäki, P. & Slotte, J. P. Cholesterol interactions with phospholipids in membranes. *Prog. Lipid Res.* **41**, 66-97 (2002).

148. Souci, L. & Denesvre, C. 3D skin models in domestic animals. *Vet. Res.* **52**, 21 (2021).

LIST OF PUBLICATIONS

[1] Tsuchida, K., Iwasa, T. & Kobayashi, M. Imaging of ultraweak photon emission for evaluating the oxidative stress of human skin. *J. Photochem. Photobiol. B.* **198**, 111562 (2019).

[2] Tsuchida, K. & Kobayashi, M. Oxidative stress in human facial skin observed by ultraweak photon emission imaging and its correlation with biophysical properties of skin. *Sci. Rep.* **10**, 9626 (2020).

[3] Tsuchida, K. & Kobayashi, M. Ultraviolet A irradiation induces ultraweak photon emission with characteristic spectral patterns from biomolecules present in human skin. *Sci Rep.* **10**, 21667 (2020).

ACKNOWLEDGEMENTS

I am deeply grateful to Prof. Masaki Kobayashi (Graduate Department of Electronics, Tohoku Institute of Technology) for giving me the opportunity to start my research and achieve success in a series of these studies. I would also like to express my sincere appreciation for laboratory member Torai Iwasa (Tohoku Institute of Technology) for his technical assistance.

I am deeply grateful to Prof. Yoshiaki Yamano (Faculty of Agriculture, Joint Department of Veterinary medicine, Tottori University) who is a chief supervisor of my doctoral thesis. He gave me a great opportunity with my doctoral thesis and invaluable advice and comments. I am deeply grateful to Prof. Toshio Ohta, Prof. Yoshiaki Hikasa, Prof. Takashi Takeuchi (Faculty of Agriculture, Joint Department of Veterinary medicine, Tottori University) and Prof. Akikazu Fujita (Basic Veterinary Science, Joint Faculty of Veterinary Medicine, Kagoshima University) for peer reviewing the manuscript for my doctoral thesis as assistant supervisors.

I would like to thank Dr. Jiro Kishimoto (Shiseido Global Innovation Center; current institution: Hayashibara Co.,Ltd.) for his invaluable support and sincere encouragement. I would like to thank Dr. Hirofumi Aoki and Dr. Yuzo Yoshida (Shiseido Global Innovation Center) for their support.

Last of all, I would like to express my heartfelt gratitude to my family for their support.